



Enhancing Polymer Matrix Reinforcements: Exploring the Potential of Biologically Modified Clay Minerals in Dyeing, Pigment Dyes, and Wastewater Treatment

Sara A. Ebrahim ^a, Ahmed G. Hassabo ^{b*}, and Hanan A. Othman ^a

^a Benha University, Faculty of Applied Arts, Textile Printing, Dyeing and Finishing Department, Benha, Egypt

^b National Research Centre (Scopus affiliation ID 60014618), Textile Research and Technology Institute, Pre-treatment and Finishing of Cellulose-based Textiles Department, 33 El-Behouth St. (former El-Tahrir str.), Dokki, P.O. 12622, Giza, Egypt

Abstract

In recent decades, a great deal of study has been done on the use of biologically modified clay minerals as polymer matrix reinforcements. The most popular method for creating organophilic clay is the ammonium surfactant-cation exchange reaction. However, the clay minerals and polymer matrices are not effectively joined by a covalent link created by this type of surface alteration. To establish compatibility and good dispersion between the hydrophilic clay and hydrophobic polymer, a wide range of silane coupling agents has been used. When compared to raw polymers, the resulting polymer/organoclay nanocomposites show notable improvements in their mechanical and physical characteristics. This paper exposures composition, kinds, characteristics, and uses of clay in the fields of dyeing, pigment dyes, and removal of Wastewater.

Keywords: Clay, Types, Nanocomposite, Application

Introduction

The textile sector is making a significant contribution to environmental safety by creating and supplying safe materials and products. Functional fabrics have been around since the late 1980s. The goal of these fabrics is to incorporate a variety of qualities and increase their performance. Textile innovation has surged in recent years, surpassing expectations. In a short period of time, the textile sector experienced significant advances[1].

Polymer matrix-based nanocomposites have lately emerged as a potential area of current global research due to the explosion of nanotechnology. These novel materials are generating a lot of attention for a variety of industrial uses, primarily in the building and construction, transportation, and food packaging plastics sectors[2]. Compared to clean polymers, they frequently display exceptional qualities such as distinct mechanical and electrical conductivity, strong gas and liquid barriers, flame retardant, and thermal characteristics[3-5].

Clay Definition

Clay is a cheap substance, referring to an inexpensive natural raw material that has been widely used as a filler for plastics and rubber since it helps to lower the price of these manufactured polymeric products. The vast majority of clay minerals fall into the category of layered silicates, also known as phyllosilicates, which are ultimately caused by the proportionate arrangement of silica or alumina sheets. Clay is made up of silicate-layered sheets with lateral dimensions of 200–300 nm and 1 nm in thickness[6]. Clay's layered silicate structure consists of 2-D arrays of silicon-oxygen tetrahedral and magnesium or aluminum-oxygen/hydroxyl/octahedral units[7]. Layered silicates, whether natural or synthetic, are composed of stacks of alumina-silicate layers with a high aspect ratio and large surface area. Layered silicates are readily available at affordable costs. Clays layered silicates are now the most common employed in the development of polymer nanocomposites[8].

* Corresponding author: Ahmed G. Hassabo, E-mail: aga.hassabo@hotmail.com, Tel. 00201102255513

Received date: 11 May 2024, **Revise Date:** 02 June 2024, **Accept Date:** 26 June 2024

DOI: 10.21608/jtcp.2024.288767.1371

©2025 National Information and Documentation Center (NIDOC)

Types of Clay

In generally, the various kinds of clay minerals are essentially made up of alternating of tetrahedral silica sheets "SiO₂" and alumina octahedral layers "AlO₆" in ratios of 1:1 if one octahedral sheet is attached to one tetrahedral sheet as Kaolinite, Halloysite, or in ratios of 2:1 this structure created from two tetrahedral sheets sandwiching an octahedral sheet such as Montmorillonite and Sepiolite, finally the proportion of 2:1:1 (chlorite), this latter are not a One side of this lamella remains linked to each other via shared oxygen atoms, as seen in Figure 1.

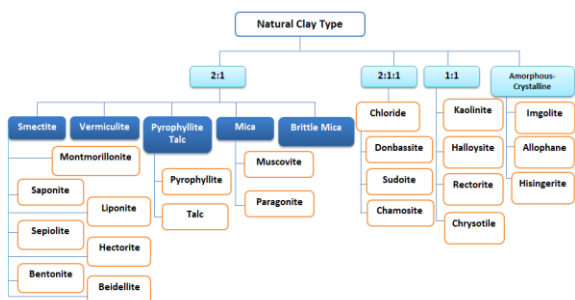


Figure 1: Natural Types of Clay

Montmorillonite (MMT)

Montmorillonite (MMT) (Figure 22 and Figure 3) is a popular layered silicate employed to create polymer/layered silicate nanocomposites. It belongs to the 2:1 phyllosilicate family. MMT has a high surface area (800 m²/g) and aspect ratio (100-200), leading to effective reinforcing potential. In general, gallery surfaces are treated with cationic surfactants to ensure compatibility with the polymer matrix. For nonpolar rubbers like ethylene-propylene (EP), ethylene-propylene-diene rubber (EPD), butadiene rubber (BR), isoprene, isoprene rubber (IR), styrene-butadiene rubber (SBR), and natural rubber (NR), a nonpolar ammonium cation, such as hydrogenated tallow, is preferred. Polar rubbers, such as Butadiene-acrylonitrile (NBR) and devulcanized bromobutyle (BIIR), benefit from a more polar hydroxyethyl substituent[8].

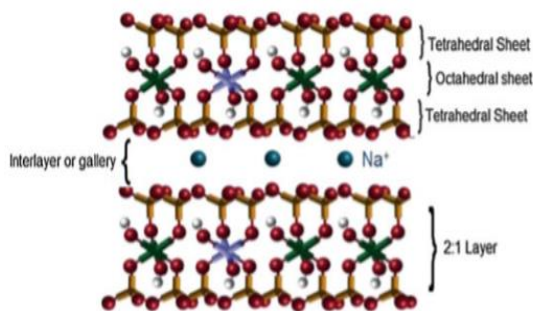


Figure 2: Structure of Na-MMT

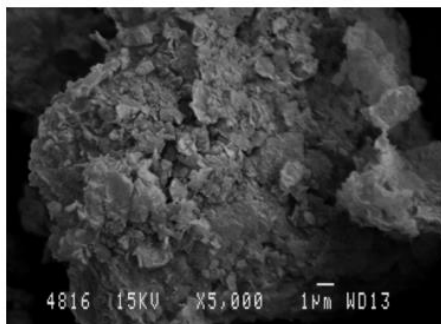


Figure 3: Montmorillonite (MMT) SEM

Zeolite

One common material used to cleanse wastewater is natural zeolite see Figure 4. The chemical formula for the dehydrated zeolite is $[Al_{12}Si_{12}O_{48}]^{12-}$ [9]. It exhibits a very peculiar behavior because of its several unique features (such as porosity, surface area, permeability, and CEC). Its elevated specific surface areas range from 200 to 860 m² g⁻¹[10-12]. Its treated natural zeolite has a particle size ranging from 1 to 12 µm. Its specific surface varies greatly and can be significantly increased by alterations. Its density is roughly twice that of water. For instance, nitric acid treatment of clay can be used to enhance its surface since it reduces the amount of aluminum in its structure, making it less crystalline and increasing the specific surface area[13]. When examining its electric charge, it can be seen that during the proton exchange process, both the overall electric charge and the quantity of cations in the zeolite skeleton remain rather stable in aqueous solution. Approximately 563 cmol·kg⁻¹ is its CEC. Zeolite, on the other hand, has a high absorption capacity since the electric field in the crystal varies and a different number of ions are exchanged during this process. Ion movement is facilitated by the zeolite's unique channels and pores, which also increase the ions' ability to adsorb[14-16].

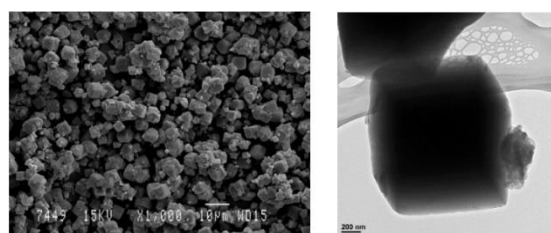


Figure 4: Zeolite SEM (left) and TEM (right)

There are two types of zeolites that are used: synthetic and natural. It is important to note that natural zeolites have non-uniform crystal sizes due to the presence of various impurities, but synthesized zeolites are incredibly pure and have uniformly sized crystals. Zeolites also form differently: while they can be synthesized in a lab in a matter of hours or days, natural zeolites can take days or years to form.

Additionally, zeolites have a very uniform crystal size, and their pore size can be controlled by designing them in accordance with specified requirements[17]. Synthetic zeolites can be produced and used as both artificial and natural elements. However, this does not mean that any element is cost-effective to synthesize. The most commonly utilized processes include hydrothermal[18], alkali-leaching[19], and sol-gel[20]. Each approach is used to obtain the appropriate zeolite type. Clearly, it is vital to consider each method's limitations and advantages. Limitations of nanoclays include non-reverse adsorption and steric blocking for secondary elements. Adsorption of large molecules is challenging due to their porosity[21]. The scientists found that zeolite may adsorb up to 99% Ni (II), a typical pigment component, in basic or neutral mediums[22]. The scientists combined zeolite b and TiO₂ to adsorb up to 99% Cd (II) in any pH solution see Figure 5[23].

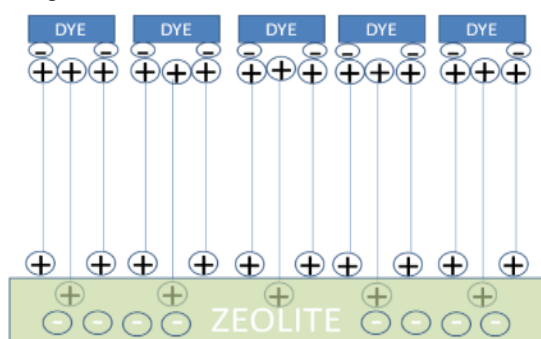


Figure 5: Zeolite adsorption of dye

Halloysite

Halloysite is a 1:1 clayey that occurs naturally and is considered a biocompatible substance. Halloysite nanotubes range from 40-70 nm in diameter and 200-2000 nm in length see Figure 6 [24]. The authors determined the specific surface area (SSA) of 47 m²·g⁻¹ and the CEC of 9.45 cmol·kg⁻¹ see Figure 7[25]. The interstratified phases are high-charge halloysite-smectite mixed-layered clays (CEC, 30-72 cmol/kg clay)[26]. Their exterior surface is negatively loaded and made of SiO₂, whilst their inner area is positively loaded and made of Al₂O₃. Halloysite nanotubes (HNT) have gained popularity due to its cylindrical shape and unique qualities, such as high surface area to size ratio, drug release, affordability, and thermal stability[27-30].

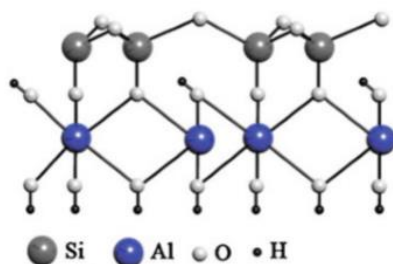


Figure 6: Chemical structure of halloysite

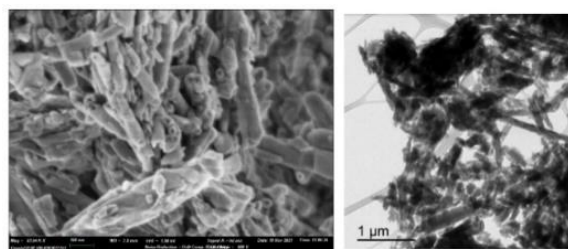


Figure 7: Halloysite SEM (left) and TEM (right) images

To explain its aforementioned properties, HNT relates to the aluminosilicate's family, having one octahedral aluminum oxide layer alternating with another tetrahedral silica layer. This mismatch between the two specified layer types results in a feature. HNTs are categorized as aluminosilicates, with alternating octahedral aluminum oxide and tetrahedral silica layers. The mismatch between the two layer types creates a hollow tubular structure for the nanoclay, giving it unique features due to its nanoarchitecture[31]. The properties of HNTs are mostly determined by their geological deposit, as discussed in the literature[32]. Their biocompatibility makes them ideal for adsorbing dyes [33, 34] like methylene blue (MB)[35-41], azo dyes[42-45], triaryl and diaryl methane dyes, and xanthine dyes, as well as adsorption of heavy metals[46-55]. A study found that combining halloysite with ZnO nanoparticles and photocatalytic degradation effectively removed Orange G from both simulated and real water. Up to 94% of the dye was removed[56].

Saponite

Saponite (Sap) is a trioctahedral clay minerals from the 2:1-type smectites group. It consists of silicate layers interspersed with gibbsite layers in the form of silicate-gibbsite-silicate. It has negatively charged layers which are neutralized by other ions carrying positive Na⁺ and Mg²⁺ charges. Saponite has a cation exchange capacity (CEC) of 100 cmol kg⁻¹[57-60]. XRD and SEM/EDX analysis reveal that the clay mineral has the structural formula $\text{Na}^{\text{TET}}[\text{Si}_7\text{Al}]^{\text{OCT}}[\text{Mg}_6]\text{O}_{20}(\text{OH})_4$ [61]. It has a large specific surface area (SSA) and an acidic pH. The specific surface area (SSA) was evaluated using ethylene glycol monomethyl ether (100-115 m²/g). Sap is more thermally stable, has a smaller particle size (about 50 nm), and is easier to delaminate and exfoliate in nanoplate units or individual nanolayers in aqueous solution than other nanoclay minerals like MMT[62, 63]. Sap's chemical makeup changes based on the geological process that created it. These flaws may limit its applicability during adsorption procedures[64, 65].

Sepiolite

Sepiolite is a natural 2:1-type fibrous nanoclay mineral with the chemical formula $\text{Si}_{12}\text{O}_{30}\text{Mg}_8(\text{OH})_4(\text{H}_2\text{O})_4 \cdot 8\text{H}_2\text{O}$. Type 2:1 consists of

two tetrahedral silica layers interleaved with octahedral magnesium oxide layers. The morphology is similar to zeolites, with ribbon-like composites forming an open channel. The structure (approx. $0.4 \text{ nm} \times 1 \text{ nm}$) can be formed through organic and inorganic cation penetration. The sepiolite surface contains many silanol (Si-OH) groups due to a discontinuous silica sheet on the outer 2:1 layers see Figure 8 and Figure 9 [66, 67].

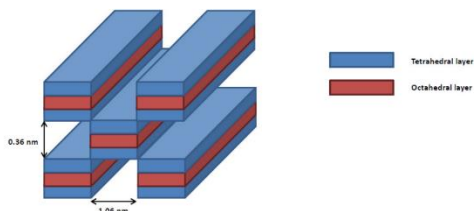


Figure 8: Sepiolite Type 2:1 two tetrahedral silica layers, and another octahedral

The sepiolite composition has three modification/adsorption zones: SiOH groups along the fiber axis, oxygen ions in the tetrahedral silica layers, and cationic exchange gaps. Sepiolite's adsorption capacity is also affected by the substance's load, shape, and size. Scientists have discovered that low-polarity and big molecules can't penetrate sepiolite channels and only account for around 40% of total SSA, despite being adsorbed on the tetrahedral silica layer [68]. Unlike MMT, organic modifiers can be added to the sepiolite surface at concentrations ranging from 400 to $500 \text{ m}^2 \cdot \text{g}^{-1}$ [69].

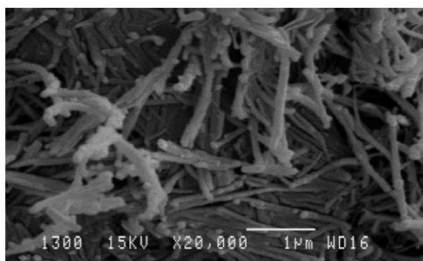


Figure 9: . Sepiolite SEM

The pH parameter is crucial since it influences sepiolite adsorption capability. Due to isomorphous nanoclay substitutions, their structural charge may be charged by pH, resulting in hydroxyl dissociation [70].

Bentonite

Bentonite (BTE) is an aluminosilicate composed of one octahedral aluminum oxide layer and two tetrahedral silicon oxide layers, yielding a 1:2-type structure with the chemical formula $\text{A}_{12}\text{H}_2\text{Na}_2\text{O}_{13}\text{Si}_4$. This clay is widely used as an adsorbent due to its outstanding cost-effectiveness ratio. It is also readily available throughout the world. Some writers attribute bentonites' strong adsorption ability to the

formation of an NH_4^+ group as a result of their high CEC [71-73].

Laponite

Laponite (Lap) is an inorganic stratified silicate element that is commonly utilized to enhance the rheology of many water-based goods. It reacts well with water-based components, resulting in increased viscosity when combined [74-76]. Research suggests that Lap can effectively disperse in water and enhance the dispersion of other elements in solution by preventing solid agglomeration see Figure 10 [77-79].

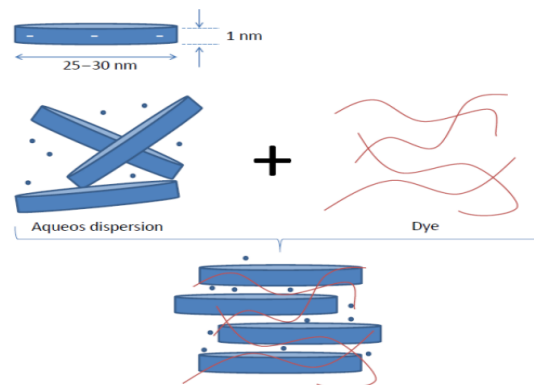


Figure 10: Laponite aqueous dispersion and dye adsorption

Synthetic Lap ($\text{Si}_8(\text{Mg}_{5.5}\text{Li}_{0.4}\text{O}_{24})^{0.7}\text{Na}_{0.7}^+$) is a 2D clay disc-shaped silicate that is around 1 nm thick. The diameter is 25 nm. The raw Laponite is predicted to have an SSA of $11.7 \text{ m}^2 \cdot \text{g}^{-1}$. It has persistent negative charges due to isomorphous substitution. Depending on the temperature, concentration, and curing time, it can create a thick gel that dissolves in aqueous solution or a translucent fluid [80-83]. In the textile sector, it can serve as an excellent pigment addition because it protects them from external elements such as temperature and oxygen while also improving the pigment's final durability [84-86].

Hydrotalcite

Hydrotalcite, $\text{Mg}_6\text{Al}_2(\text{CO}_3)(\text{OH})_{16.4}(\text{H}_2\text{O})$ see **Figure 11**, is classed as a nano-sized mineral due to one of its lamination dimensions being smaller than 20 nm. Because of its unique structure, it belongs to the "layered double hydroxides" (LDH) category. This layer has an SSA of $71 \text{ m}^2 \cdot \text{g}^{-1}$ to $104 \text{ m}^2 \cdot \text{g}^{-1}$ [87]. Researchers are increasingly interested in these elements for their diverse applications, including catalysts, therapeutics, and adsorption. LDH composites can adsorb anions via a variety of methods. The most common kind is caused by direct adsorption in dispersion. Adsorption of a solid is limited by its crystallinity, as well as the polarity, temperature, anion size, and pH of the surrounding medium [88].

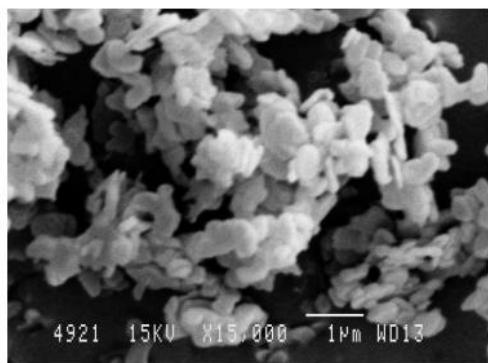


Figure 11: Hydrotalcrite SEM

Clays' Geographic Distribution

Research on soil formation indicates that temperature and meteoric changes play a role in rock erosion. The resulting components in solution move across the earth's surface and mix to form new minerals, such as clay see **Figure 12**.

In humid equatorial tropical climates, heat and rainfall expose rocks to high levels of hydrolysis. Water trickling removes a portion of the released chemical contents in the form of ions or complex ions, with the exception of iron, alumina, and silica, which remain. Iron precipitation to hydroxides results in on-site concentrations of iron hydroxides such as hematite, magnetite, and goethite. Alumina deposits in gibbsite or mixes with silica to generate kaolinite. Laterites are red soils with high levels of kaolinite, iron oxides, and gibbsite.

In a tropical-subtropical climate with alternating seasons, rock hydrolysis occurs mostly during the wet season, while ion evacuation is minimal during the dry season. Beidellite, a smectite mineral, grows under these conditions. This creates unique clay soils like "vertisoil" and "fersiallitic".

In temperate climate, Low temperatures and rainfall limit the alteration of silicate minerals, save for sensitive minerals such mica sericites, chlorite, and clay. Minerals such as vermiculite, smectite, and interstratified chlorite-Al are formed as a result of fundamental alterations.

In the boreal climate of the North Pole, Organic compounds can destroy aluminosilicates due to their acidic nature. As a result, podzol soils emerged, with ashen backgrounds and high quartz content.

In extreme, Rocks in severe, periglacial, and desert climates are resistant to change due to lack of water, organic matter, and other factors. Soils in these places are often thin and made mostly of illite and chlorite. originating from the pulverization of existing phyllosilicates.

Figure 12, illustrates the correlation between soil type and climate. This relationship is used in paleoclimatology to recreate previous climates using clay studies.

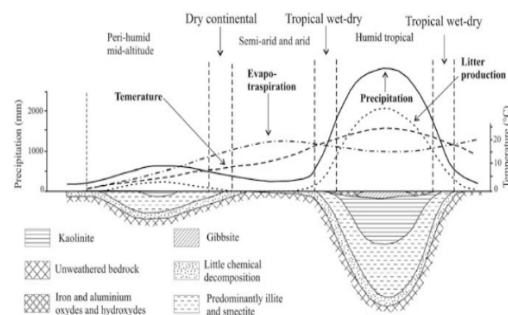


Figure 12: A representation of the link between soil type (clay mineral makeup) and climate.

The Geological Cycle of Clays

Clay minerals represent the recycling history of the lithosphere see Figure 13. The story begins if silicate minerals (quartz, feldspar, mica, pyroxene, olivine) from the earth's crust (basalt, granite, peridotite, shale) arise into contact with water (meteoric or hydrothermal). Thus, hydrolysis of silicate rocks helps to "birth" clay minerals. Wind and water currents that animate the surface then mobilize the latter. the earth to reach the sedimentary basins, including the ocean depths. Detrital clays will combine with authigenic clays generated locally through diagenesis. Clays, both hereditary and neofomed, can undergo modifications resulting in complicated sequences.

Clay deposits in the ocean's depths are buried over millions of years owing to subsidence and tectonic activity. At vast depths, where temperatures and pressures are high, the different clays (kaolinite and smectite) recrystallize during diagenesis to become illite and chlorite. Clay minerals undergo metamorphism beyond diagenesis, resulting in mineral assemblages of high temperature and pressure (mica, feldspar, etc.), indicating the "death" of clays. Metamorphism involves partial melting of materials at the crust's base, resulting in magmas that eventually rise to the earth's surface as effusive and plutonic rocks.

Clay sediments' ability to retain water affects water movement from the earth's surface to the crust, resulting from the partial fusing of meta-sediments and magma in subduction zones[89].

Geological Prospecting Clays

Natural clays are uncemented rocks that occasionally get compacted. They can range in color from white to red or green and exhibit diverse patterns of deposit (in clusters, lenses, or layers of different thicknesses) depending on their genesis and origin. Geological, geotechnical, and theme maps, along with other works and regional geological studies, can direct exploration efforts in each nation toward regions with abundant deposits of clays with varying geological ages and petro-mineralogical characteristics.

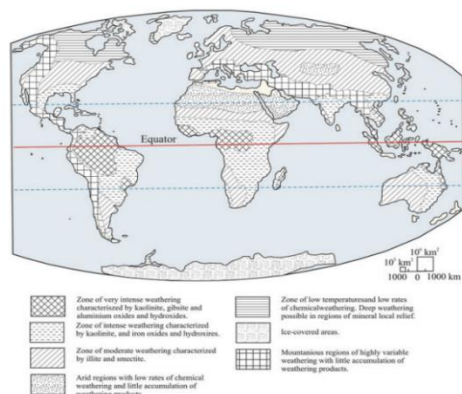


Figure 13: Synthetic Scheme of the distribution of clay minerals on the surface of the continents

Using the case of Morocco to demonstrate the spatial distribution of clay deposits at the national level. Morocco has great geographical and structural diversity due to its location at the northwest tip of Africa and a short distance south of Europe **Figure 14**. From Archean to Quaternary, all rock types are represented, and they all still bear the memory effects of the tectono-metamorphic processes that their various orogenesis underwent. Alpine, Hercynian, Caledonian, and Pan-African[90, 91].

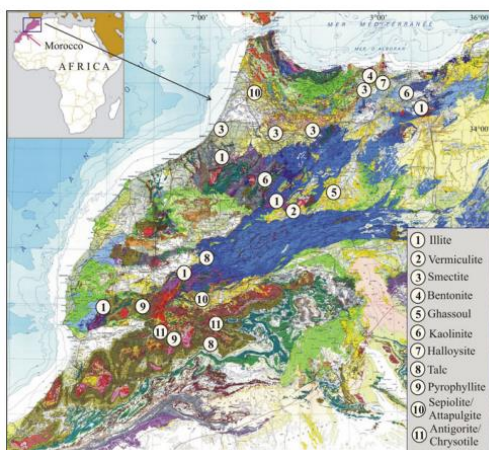


Figure 14: Geological map of Morocco (Northern provinces) indicating the spatial distribution of the main types and clay deposits. (1 Illite; 2 Vermiculite; 3 Marl; 4 Bentonite; 5 Ghassoul; 6 Kaolinite; 7 Halloysite; 8 Talc; 9 Pyrophyllite; 10 Sepiolite and Attapulgite; 11 Antigorite and Chrysotile)

Structure of Clay

The layers are divided into two types: tetrahedral sheets with four oxygen atoms around a silicon atom, and octahedral sheets with eight oxygen atoms surrounding a metal such as aluminum or magnesium. The tetrahedral (T) and octahedral (O) sheets are joined together by sharing oxygen atoms. Hydroxyl form has unshared oxygen atoms. Clay has a one-layer structure formed by fusing tetrahedral and octahedral sheets together see Figure 15[92].

- The typical composition of the kaolin group is $Al_2SiO_5(OH)_5$, which is one tetrahedral fused to one octahedral (1:1).
- Phyllosilicates with one octahedral sheet nested between two tetrahedral sheets (2:1)[93].

Each platelet can be roughly 1 nm thick, with lateral dimensions ranging from 30 nm to several micrometers or even larger, depending on the silicate, due to an isomorphous replacement of alumina cation (Al^{3+}) within the layers. For example, in the case of 2:1 structure, the trivalent Al-cation in the octahedral layer is partially substituted by the divalent Mg-cation to produce the Montmorillonite structure, giving each layer a net negative charge caused by the distinction in valence. The negative charge is counterbalanced by the interlayer alkali or alkaline earth metal cation as sodium and calcium ions. If these charges are not balanced and these ions do not fit in interlayer space, the mica will be formed and/or the layers organize themselves to form clay stalks and held together by relatively weak bonding forces of attraction between them as van der Waals force, interstitial water and other polar molecules can be placed inside the galleries.

The interlayer space of every kind of expandable clay is determined by the size and sort of charge compensating cation and polar molecules on interior surfaces within the crystal clay structure itself; the presence of them on the basal plane renders the clay hydrophilic in nature. Expansion of the space between two consecutive layers, known as interlayer space, imparts significant cation exchange capacity (CEC) relative to non-expandable phyllosilicates and the majority of secondary minerals see Figure 16 [94].

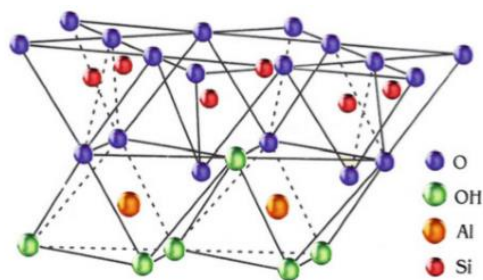


Figure 15: Clay structure

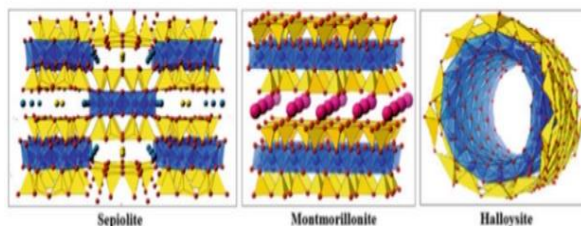


Figure 16: Clay structures (nano-fibers, plate-like filler, and nano-tubes)

Cation Exchange Capacity (CEC) is determined to be an approximation of the number of readily exchangeable cations in the clay that neutralize negative charge see Figure 17. Otherwise, it designed the clay's capacity to store cations such as A^{13+} , Ca^{2+} , Mg^{2+} , Mn^{2+} , Zn^{2+} , Cu^{2+} , Fe^{2+} , Na^+ , K^+ , and H^{+14} , which was previously stated as milliequivalents per 100 g (meq/100 g). The CEC value varies from clay to clay[95]. A comparison of CEC values for various clay types is provided in Table 1

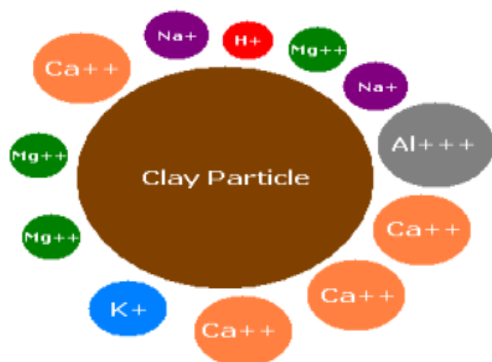


Figure 17: Clay Particle Surrounded by Different Cations

Nomenclature and Classification

The most important property of clays is their layered structure. Clays are inorganic compounds formed from stacked layers. Iono-covalent bonds connect atoms in stacked layers in a perpendicular direction, using weaker pressures. Layers can be separated with minimal energy, but breaking them requires far more energy. Clays are a sub-family of the layered oxides (oroxyhydroxides). They are not all silicates; several are free of any silicon atoms. Clays used to create polymer nanocomposites are primarily silicates[93].

Clays are classified based on the layer's electrical charge, as demonstrated in Table 2. Positively and

negatively charged layers are balanced by an equal number of opposite charges in the interlayer region. Clays with negative and positive charges are referred to as cationic and anionic, respectively.

Silylation of Clay Minerals

Lately, silane grafting, also known as silylation, has shown to be a successful method of altering the surfaces of clay minerals. However, by simply grafting hydrophobic silane groups onto the clay minerals, the interaction between hydrophobic molecules and clay might be significantly improved. The resulting silylation compounds show potential for use in material science, particularly in polymer/clay nanocomposites see Figure 18 [96].

In general, silane coupling agents interact with clay minerals through a series of processes as seen in Figure 19. At first, the silane monomers react in the presence of water (hydrolysis) to form reactive, hydrophilic, acidic silanol groups Si-OH, followed by partial condensation in which oligomers are formed; during the condensation, silane molecules react with one another to form dimers, which then condense to form siloxane oligomers. After that, the oligomers or monomers silanol are physically adsorbed to the hydroxyl groups of clay minerals via hydrogen bonding on the clay surfaces. Finally, during the dehydration condensation reaction, a strong covalent link -Si-O-Si- is generated between silanols and clay hydroxyl groups during the drying phase[97, 98].

Furthermore, the covalent link stabilizes organic moieties in silane-grafted products, preventing them from leaking into surrounding fluids. Additionally, the R' organofunctional group can react with the polymer matrix, creating a network of covalent connections between silane, clay mineral, and polymer. As a result, the polymer/clay nanocomposite demonstrates a significant improvement in various properties, including mechanical, rheological, and other handling qualities [107-110].

Table 1: Ranges of cation exchange capacities for clay

Type of Clay	Structure Type	CEC (meq/100g)	d-spacing (Å)	Chemical Formula	Ref
Kaolinite	1:1 (TO)	3-15	7.14	$[Si_4]Al_4O_{10}(OH)_8.nH_2O$ (n=0 or 4)	[99]
Halloysite	1:1 (TO)	5-50	7	$[Si_4]Al_4O_{10}(OH)_8.nH_2O$ (n=0 or 4)	[100]
Illite	2:1 (TOT)	10-40	10	$M_x[Si_{6.8}Al_{11.2}]Al_3Fe_{0.25}Mg_{0.75}O_{20}(OH)_4$	[101]
Chlorite	2:1:1 (TOT)	10-40	14	$(Al(OH)_{2.55})_4[Si_{6.8}Al_{11.2}] Al_{13.4}Mg_{0.6}O_{20}(OH)_4$	[94]
Montmorillonite	2:1 (TOT)	60-150	12.4	$M_x(A_{14-x}Mg_x)Si_8O_{20}(OH)_4$	[102]
Vermiculite	2:1 (TOT)	100-150	9.3-14	$M_x[Si_7Al]Al_3Fe_{0.5}Mg_{0.5}O_{20}(OH)_4$	[103]
Hectorite	2:1 (TOT)	120	12.4-17	$M_x(Mg_{6-x}Li_x)Si_8O_{20}(OH)_4$	[104]
Saponite	2:1 (TOT)	86.6	12.4-17	$M_xMg_6(Si_{8-x}Al_x)Si_8O_{20}(OH)_4$	[105]
Sepiolite	2:1 (TOT)	11-12	12	$Mg_4Si_6O_{15}(OH)_{2.6}(H_2O)$	[106]

Table 2: Clays are classified based on their electrical charge.

Type of Layers	Type of clay	Main features
neutral layers	pyrophyllite, talc, kaolinite	Neutral clays, layers connected by vander Waals interactions and/or hydrogen bonding.
negatively charged layers	phyllosilicates:e.g. bentonites(main component: montmorillonite)	Cationic clays compensate for negative layer charge with interlayer cations.
Positively charged layers	hydrotalcite (HT). layered double hydroxides (HT-like family)	Anionic clays compensate for positive layer charge using anions in the interlayer space.

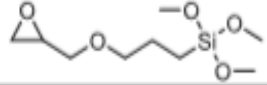
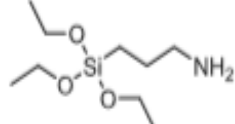
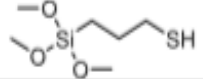
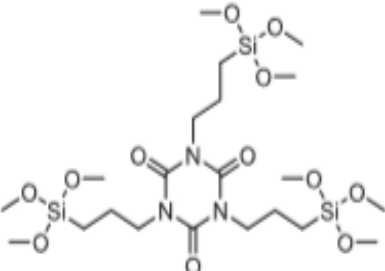
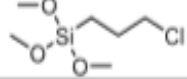
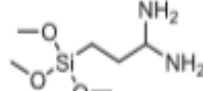
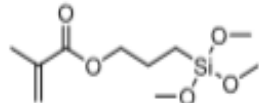
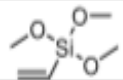
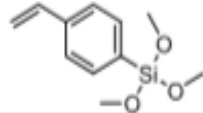
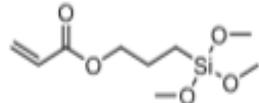
Functional group	Chemical name	Structural formula
Epoxy	3-Glycidoxypropyltrimethoxysilane	
Amino	3-Aminopropyltriethoxysilane	
Mercapto	3-Mercaptopropyltrimethoxysilane	
Isocyanate	Tris-(trimethoxysilylpropyl) isocyanurate	
Chloroalkyl	3-Chloropropyltrimethoxysilane	
Diamino	Diaminopropyltrimethoxysilane	
Methacryloxy	3-Methacryloxypropyltrimethoxysilane	
Vinyl	Vinyltrimethoxysilane	
Styryl	<i>p</i> -Styryltrimethoxysilane	
Acryloxy	3-Acryloxypropyl trimethoxysilane	

Figure 18: Some Commercial silanes coupling agents with different organofunctional groups

Organo-clays

Clays have been known to benefit from surface treatment for many of the past several decades. As a result, the inorganic cations (such as Na⁺ and K⁺) that were initially present on the clay surfaces are replaced when an amine salt or quaternary ammonium salt is added to a clay-water suspension see Figure 20. The amino groups are anchored on the clay surface as a result of this exchangeable adsorption, and the hydrocarbon tail is positioned in the gallery space, pushing the water molecules that have

previously been adsorbed. The clay is referred to as organophilic since it can now coexist with organic molecules[111].

Organo-clay structures and modelling

On the gallery surfaces of smectite clays, the substitution of organic onium ions for inorganic exchange cations not only broadens the clay galleries but also aligns the polarity of the clay surface with that of the polymer.

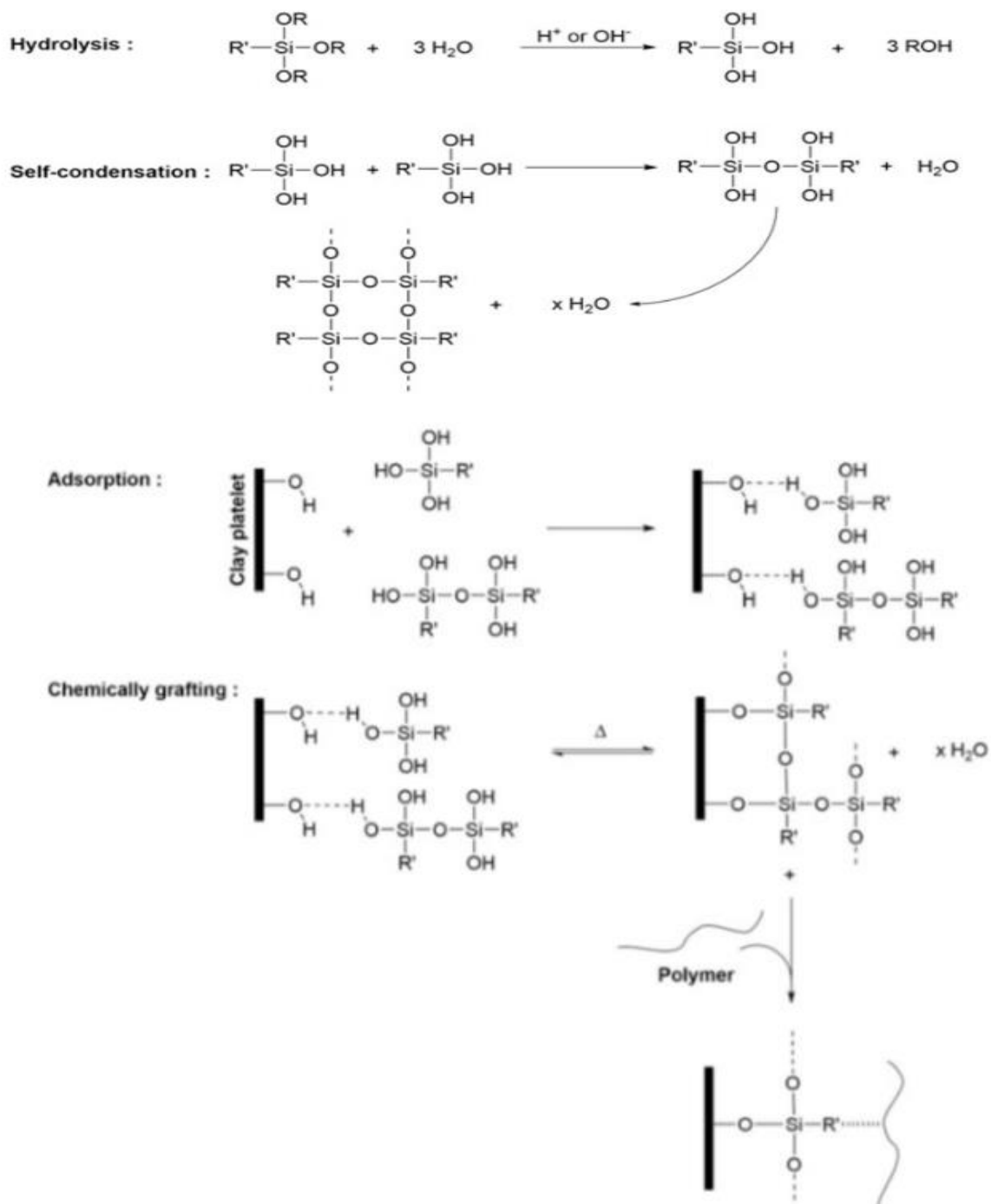


Figure 19: A plausible mechanism of coupling reaction between silane grafted clay mineral and thermoplastic matrices

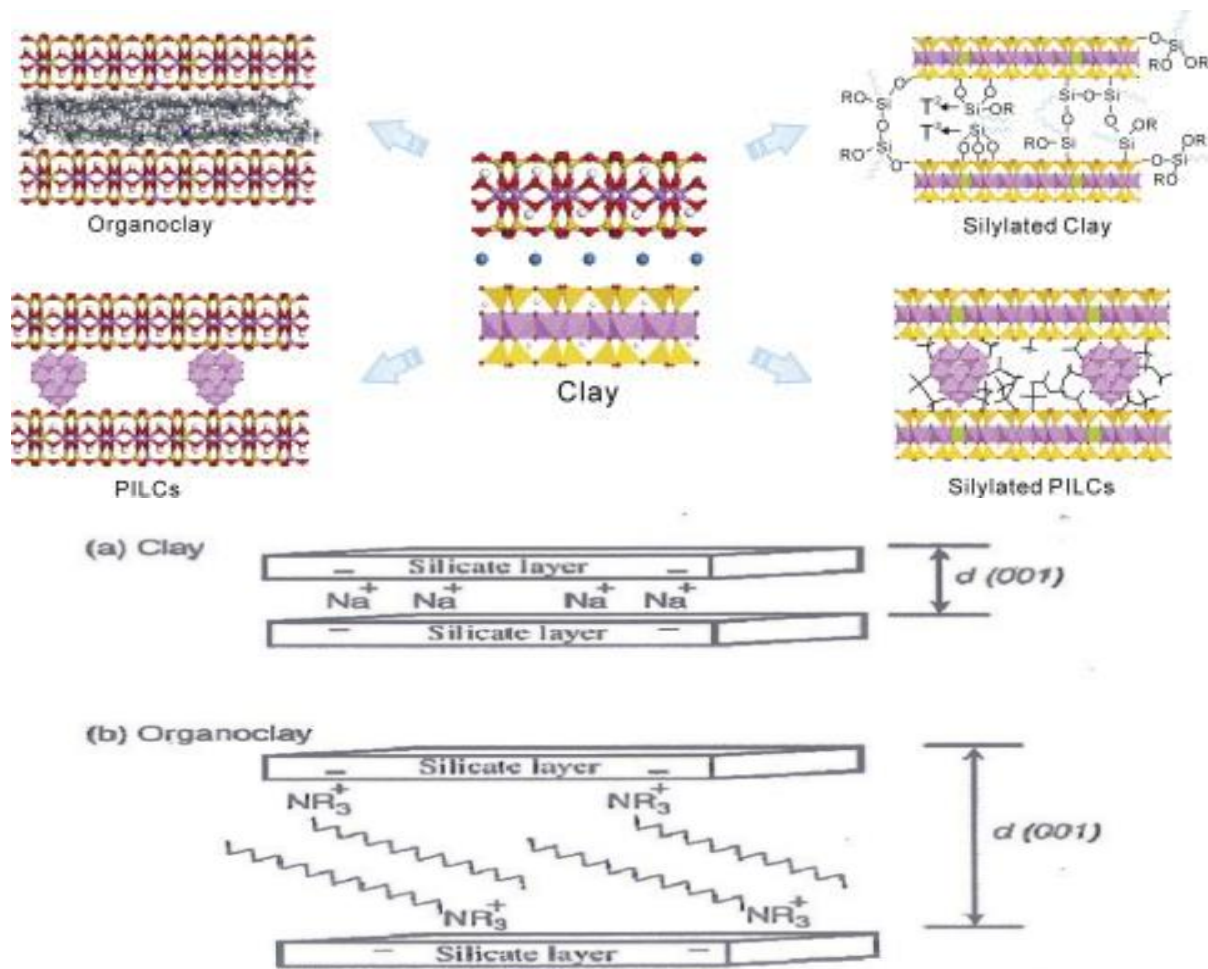


Figure 20: Scheme of clay and its modified (a) clay and (b) modified clay



Figure 21: Preparation of organoclay

This either makes it easier for preformed polymer or polymer precursors to enter the gallery area (intercalation). Different configurations of the onium ions are possible depending on the charge density of the onium ion surfactant and clay. The clay layers will generally be driven farther apart the longer the surfactant chain length and the greater the clay's charge density. This makes sense because the intragallery surfactant occupies a larger volume as a result of both of these characteristics. The onium ions may lie parallel to the clay surface as a monolayer, lateral bilayer, pseudo-trimolecular layer, or tilted paraffin structure, depending on the charge density of the clay. Large surfactant ions have the ability to adopt lipid bilayer orientations in the clay galleries at very high charge densities.

Organo-clay synthesis

By substituting alkyl ammonium or alkyl phosphonium (onium) cations for the sodium and calcium cations found in the inter-layer space or clay galleries, organoclays can be synthesized via a cation exchange method. Alkyl ammonium or alkylphosphonium cations are inserted into the galleries to modify the clay layers' surfaces and increase their hydrophobicity. This also results in a slight increase in inter-layer spacing, which encourages the subsequent intercalation of polymer chains into the galleries during the preparation of nano composites. Furthermore, functional groups that engage with polymer chains or start polymerization can be provided by the alkylammonium or alkyl phosphonium cations, which increases interfacial contacts. The most common methods for preparing the organo-clays in solutions are cation exchange reaction or by solid-state reaction [112, 113].

Morphology

Most clay minerals are sandwiches of two structural units: tetrahedral and octahedral. The simplest sort of sandwich is made of a single layer of silica tetrahedral with an aluminum octahedral layer on top: they are known as 1:1 mineral sand and belong to the kaolinite family. The other major type of sandwich is the 2:1 structure (smectite minerals), which is made up of an octahedral filler sandwiched between two tetrahedra. The octahedral positions in smectite minerals can be inhabited by magnesium, iron, or tiny metal ions, in addition to aluminum. Montmorillonite clay minerals are widely used in nanocomposites due to their tiny size of particles (< 2 μ m) and ease of polymer dispersion. They also have high aspect ratios (10-2000) and a significant swelling capacity, that's necessary for efficient polymer intercalation[114].

Compatibilizing Agents

Dispersing clay in a polymer is similar to mixing oil and water. Oil does not disperse effectively in

water, except in the presence of detergent. A compatibilizing agent serves a similar purpose as a detergent. It is a molecule made up of two functions: one hydrophilic (which prefers polar media such as water or clay) and one organophilic. In the case of detergents, this allows for the dispersion of oil in water and clay in polymers. Except for water-soluble polymers, most inorganic additions are incompatible with the polymer matrix. To improve compatibility, inorganic additives must be biologically changed, such as by utilizing organic surfactants. Organic surfactants in organically modified additives serve a key function in decreasing the inorganic host's surface energy, enhancing wetting properties, and miscibility with the polymer matrix [115-117].

Natural clays' ability to adsorb organic molecules is determined by their physical and chemical characteristics. If organic molecules react strongly with hydrophilic clays, the clay layers will attract the molecules. Montmorillonite and other layered silicate clays are naturally hydrophilic, which means they are incompatible with most polymer compounds. Furthermore, clay alteration makes it more compatible with an organic matrix by exchanging ions between the clay's alkali cation and nearly any other cation. Amino acids were the original compatibilizing agents utilized in the manufacture of nanocomposites (polyamide 6-clay hybrids). Since then, a wide variety of additional compatibilizing agents have been employed in the creation of nanocomposites. Due to their ease of exchange with the ions located between the layers, alkyl ammonium ions are the most widely used. Because silanes can react with the hydroxyl groups that may be found at the clay layers' edges and/or surface, they have been employed[118, 119].

Types of polymer-clay nanocomposites

Polymer-clay nanocomposites have gained popularity owing to the observation which adding layered silicate materials (e.g. montmorillonite, hectorite, bentonite) at low loading levels (typically 3–5%) improves mechanical properties, barrier properties, and fire retardancy of polymers[120].

Polymer-clay interactions, also known as polymer-layered silicates, are the most frequent type of nanocomposites and were extensively explored in the 1960s and 1970s. Although Blumstein initially reported on this technique in 1961, true exploitation began in the 1990s, when Toyota researchers discovered how to make a nanostructure out of polymer and organophilic clay. The novel material based on polyamide 6 and organophilic montmorillonite shown significant advantages in mechanical, barrier, and thermal properties compared to the pristine matrix, even with a low clay concentration (4wt%)[121].

Since then, polymer-clay composites have been categorized into three broad categories:

- Conventional Composite (immiscible or microcomposites), where the clay functions

more like a micron-sized filler and isn't nanodispersed,

- Intercalated nanocomposite, where the layers of clay stay in register and the clay is entirely nano-dispersed
- Delaminated nanocomposite or exfoliated nanocomposite, which also exhibit high nano-dispersion and the loss of the clay layer registry should result in the most notable modifications to the mechanical and physical properties[122-124].

It is possible to create an additional category that distinguishes between intercalated nanodispersion and fully exfoliated nanocomposites. We refer to these as highly delaminated nanocomposites[125]. Clay layers are evenly distributed as 1 nm thick, non-interacting clay layers in totally exfoliated nanocomposites. Nonetheless, stacks of roughly two to twenty layers of clay are evenly distributed throughout the polymer matrix in highly delaminated nanocomposites. In this kind, stacked layers are still there, but the ordered structure's XRD peak vanishes see Figure 22 [126, 127].

Polymers Used in the Synthesis of Nanocomposites

Over the past 15 years, a wide variety of polymers have previously been employed to create polymer-clay nanocomposites through the intercalation and delamination of organophilic clays in various polymeric media. There are two sections to these polymers. **First**, Thermosets are used in nanocomposites made of polyurethanes, unsaturated polyester, and epoxies. Furthermore, the synthesis of nanocomposites has been effectively accomplished with silicone rubbers.

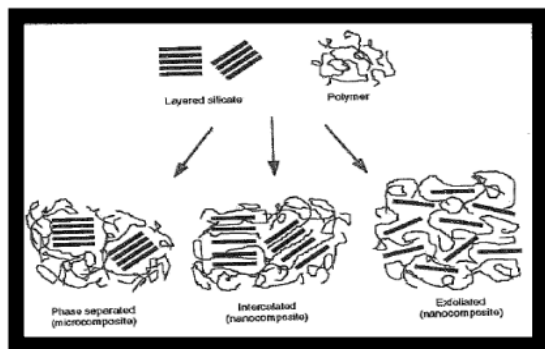


Figure 22: Possible polymer layered silicate structures

Second, thermoplastics are used in nanocomposites in the following ways: Polyamide 6 has been the earliest and most extensively researched thermoplastic used in the manufacture of polymer-clay nanocomposites. Since then, several techniques have been employed to create polymer-clay nanocomposites using other thermoplastics, including poly(ethylene oxide), poly(methyl methacrylate), polybutadiene-acrylonitrile, polydiacetylene, poly (α -

caprolactone), polystyrene, polyimide, and poly(ethylene terephthalate)[128].

Synthesis of Polymer-Clay Nanocomposites

Not all mixtures of polymers and inorganic additives will result in nanocomposites; the interfacial characteristics and compatibility of the polymer matrix and inorganic additives greatly affect the fundamental features of the materials. Kawasumi et al have created nanocomposites using a variety of polymers, including acrylic, nylon 6, polyimide, epoxy resin, polystyrene, and polycaprolactone. However, there are only a few instances in which silicate layers could be homogeneously dispersed and exfoliated, such as in polymers containing polar functional groups like amides and imides[129].

This is because polymers having polar function groups are compatible with silicate layers of clay, which include polar hydroxyl groups. Naturally hydrophilic, silicate clay layers are held together by a layer of Na^+ or K^+ ions. The typically hydrophilic silicate surface becomes organophilic through ion exchange reactions with cationic surfactants, such as primary, tertiary, and quaternary ammonium ions. This allows for the intercalation of several engineering polymers. Alkyl ammonium cations play a key role in the organosilicates by reducing the inorganic host's surface energy, enhancing their wetting properties, and enhancing their miscibility with the polymer[130].

The formation of nanocomposites can be achieved through four primary methods: Synthesis of in situ templates, methods of polymerization; solvent-based mixing and melt blending see Figure 23 [131-134].

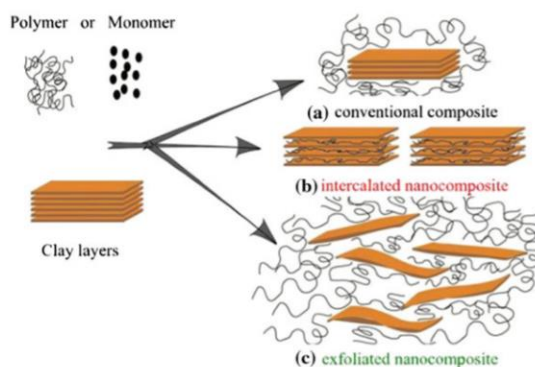


Figure 23: Schematic diagram showing synthesis of different types of polymer clay nanocomposites

Pre-Swell or Exfoliate

In this process, PCN are synthesized using a solvent such as water, acetone, N,N-dimethylformamide, toluene, or chloroform. The clay is allowed to pre-swell, or exfoliate, in a suitable solvent before being added to a polymer suspended in the same solvent. When the layered silicate is distributed in a polymer solution, the polymer chains interact and

displace the solvent within the silica gallery[104]. The intercalated nanocomposite is created, and the solvent is removed using moderate heating or vacuuming. Large volumes of volatile solvent are required for this method. It has been shown that the rise in entropy caused by solvent molecule desorption acts as a driving force for polymer intercalation from solution. This approach has been used to intercalate water-soluble polymers like poly(ethylene oxide) and poly(ethylene vinyl alcohol) between clay layers. This approach was used to synthesis nanocomposites made of cellulose, high-density polyethylene, polyimide, and other materials. The main advantage of this approach is that it allows you to create intercalated nanocomposites from polymers with little or no polarity[135-137].

The disadvantages of this process include the need for appropriate monomer/solvent or polymer solvent combinations, as well as the high prices of solvents, disposal, and environmental impact. Aranda and Ruiz-Hitzky reported the first use of this approach to create polyethylene oxide (PEO)/MMT nanocomposites. This process was utilized to make nanocomposites of nitrile-based copolymer and polyethylene-based polymer, with organically modified MMT. This approach was used to create polysulfone (PSF)-organoclay nanocomposites [104, 138].

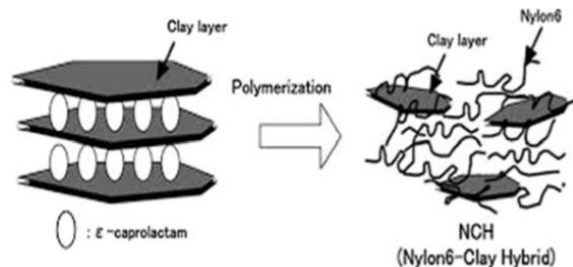


Figure 24: Schematic diagram of polymerization to NCH

In Situ Polymerization

The in situ polymerization approach has been successfully employed for nylon-6 and epoxy systems see Figure 24 and Figure 25. The modified organoclay is pre-swollen with the monomer or a monomer/solvent mixture before being activated with heat, radiation, or another suitable initiator. In 1993, Usuki et al. effectively synthesized exfoliated Nylon-6/clay hybrid (NCH) by in situ ring-opening polymerization of ϵ -caprolactam, with alkylammonium-modified layered silicate distributed beforehand[139]. Molten ϵ -caprolactam swelled organophilic clay that had been ion-exchanged with 12-aminododecanoic acid.

Messersmith et al. synthesized NCH in the same way and noticed a significant decrease in gas permeability with clay addition. In situ polymerization was also used on lactones and lactides to create polymer/clay nanocomposites. In instance, intercalative

polymerization of ϵ -caprolactone between silicate layers was described in the presence of supercritical carbon dioxide. This dry method allows for complete exfoliation of clay platelets in the matrix, which results in improved thermomechanical characteristics. Aside from polyamide and aliphatic polyester nanocomposites, the in situ polymerization process is also employed to create epoxy resins. Pinnavaia and associates described the polymerization of a liquid epoxy resin, such as diglycidyl ether of bisphenol A, in the presence of polyetheramine and organoclay.

Giannelis et al. also employed ammonium salts in which one alkyl chain has a functional group capable of reacting and bonding with the epoxy when cross-linked, such as hydroxy, epoxy, or carboxylic functional groups[140]. This causes the epoxy matrix to be directly attached to the silicate layers, increasing adhesion between the two phases and resulting in good dispersion. Polyolefins are also produced using the in situ intercalative polymerization technique. This process involves using an olefin catalyst system, such as Ziegler-Natta or metallocene, to intercalate silicate layers. Olefin is then polymerized in the presence of clay. Bergman et al.[141] pioneered this approach, using a palladium-based compound to polymerize ethylene.

In situ intercalative polymerization, particularly with clay modified to encourage polymer grafting or growth from the clay surface, is the most effective process for ensuring individual exfoliation of clay layers in the final nanocomposite materials.

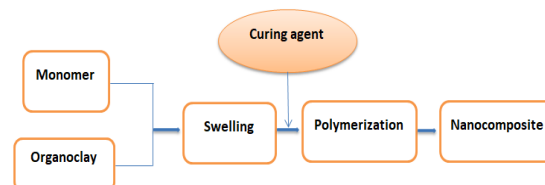


Figure 25: Different steps of the "in-situ polymerization" approach

Melt Intercalation

Melt intercalation is the third process for PCN synthesis see Figure 27 and Figure 27: Different of the "melt intercalation. Vaia et al. established this process in 1993[142]; it doesn't need a solvent; instead, a polymer matrix such as thermoplastics is combined with organoclay. However, sometimes a curing agent, such as maleated polypropylene oligomers, is necessary[143]. If the clay layer surfaces are sufficiently attractive to the polymer, the polymer can permeate between the clay layers, forming either an intercalated or exfoliated nanocomposite. Melt intercalation has been used to create nanocomposites from polyamides such as nylon 6 and nylon 66 (PA66)[144] and polyethylene terephthalate (PET). This method is preferred over others since it is simpler, less expensive, and more environmentally

friendly. The melt intercalation technology gained popularity because of its enormous potential for use in quick processing processes like injection molding and twin screw extrusion[145].

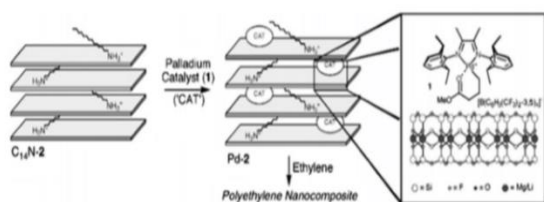


Figure 26: Polyethylene nanocomposite synthesis by in situ polymerization

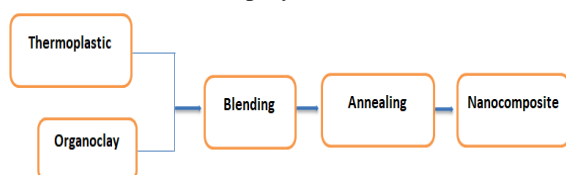


Figure 27: Different of the "melt intercalation"

Characteristics of Polymer-Clay Nanocomposites

The ability to significantly alter not only the mechanical but also some of the physical properties of the polymer through delamination of a relatively small amount of clay is the reason for the growing interest in polymer-clay nanocomposites.

With modified layered silicate contents between 2 and 10 weight percent, nanocomposites can show notable benefits over pure polymers. Improvements have been made in: mechanical qualities include tension, compression, bending, and fracture. Barrier qualities include permeability and solvent resistance. optical characteristics and ionic conductivity.

Other intriguing attributes of polymer-layered silicate nanocomposites include greater heat stability and the potential to promote flame retardancy at very low filling levels. These increased qualities are due to the production of a thermal isolating and low permeability char as a result of fire-induced polymer degradation. The Toyota research group initially found that exfoliation of layered silicates in nylon 6 significantly improved the thermal, mechanical, and barrier properties of the polymer.

The nylon 6 layered-silicate nanocomposites with a silicate mass fraction of 5% showed 40% gains in tensile strength, 68% in tensile modulus, 60% in flexural strength, and 126% in flexural modulus. Heat distortion temperature increased from 65 to 152°C. These materials are being used in motor sector applications. Following this accomplishment, the nanocomposite technology was applied to additional polymers, such as polypropylene, polystyrene, polyimide, epoxy, and unsaturated polyester resins, with comparable results[146].

Clay mineral (nm) in textiles

Clay Mineral-Polymer (nm) Composite in Textiles

Modifying fibers, enhancing fabric performance, and creating smart textiles are some of the significant textile finishing innovations made recently using particles (nm) as fillers and finish (nm) formulations. Advancements in nanotechnology of textile and fiber finishing are in the following areas see Table 4 [147]:

- Nano finishing of textile textiles and fibrous materials with a finish formulation including particles (nm).
- Fiber (nm) composites are produced using specified fillers (nm).
- The study of organic compounds that influence the performance of a chiller (nm).
- Physical and chemical optimal process control for finishing (nm) of fibrous materials.

Table 3 summarizes some of the main effects of clay mineral on fibrous polymeric materials (filament and fabric). The use of inorganic particles (nm) and their composite was viewed as an alternative antimicrobial finishing technology to avoid the toxic or damaging impacts of traditional finishes. Dastjerdian and Montazer evaluated particles (nm) of various materials such as clay mineral and clay-polymer (nm) composite, metallic and nonmetallic TiO_2 (nm) composite, carbon nanotube, silver-based materials (nm), and so on[148].

Flame retardancy was achieved by combining Mt-PU (nm) composite with polyhedral oligomeric silsesquioxanes (POSS)-PU (nm) composites. Polyester and cotton fabrics were treated with the aforementioned composites, and the coated fabric specimens were evaluated using cone calorimetry and thermogravimetric methods. Subsequently, the impacts of Mt-PU (nm) composite and POSS-PU (nm) composite were explored; however, POSS demonstrated significant flame retardant properties[149].

In special finishing, surface coating of textile might generally be used including the flame retardancy and water repellency. Polyurethane (PU) resin coatings on textile fabrics were recognized to provide water repellency and reduced air permeability. However, PU was thought to be an important study area for coating the fabric with a clay mineral-based formulation and assessing the subsequent physiological and chemical consequences. Depending on the clay mineral structure, fixing agent employed, and application process, improvements in flame retardancy and thermal stability could be achieved. A flame retardant coating incorporating branched polyethylenimine (BPEI) and sodium montmorillonite (NaMt) was developed. Four water-based coating compositions with BPEI (pH 7 and 10)

and NaMt (0.2 and 1wt.%) were applied to cotton fabrics[150].

Thermogravimetric study revealed that when heated to 500°C, coated fabric left up to 13% more char than uncoated fabric. Compared to an uncoated fabric, that amount of char was two orders of magnitude greater. In the vertical flame test, the coated cloth displayed a reduction in afterglow time. A noteworthy discovery was the retention of fiber shape and weave structure in the postburn residue of every coated cloth, as demonstrated by SEM analysis. Significantly successful was the coating mixture based on BPEI pH 7 and NaMt 1% weight content.

Microcombustion calorimeter studies revealed that coated fabrics have lower heat release capacity compared to uncoated materials. The investigation of clay mineral coated cotton fabric characteristics utilizing water-based compositions and recognized techniques has made substantial progress. Traditionally, the fiber finishing business relied heavily on water-based composition[151].

Poly(Ethylene Terephthalate (PET)) Composites

A large number of polymers were used in the form of fibers or filaments; nevertheless, the subject of modifying the behavior of polymers in fiber or filament form employing clay mineral (nm) has received little scientific attention to date. Using clay minerals (nm) to improve flame retardancy in synthetic polymer fibers such as nylon, polypropylene, polyester, and polystyrene is a challenging research topic[152].

The production of man-made microfibers via the electrospinning process has been known since the 1930s. Electrospinning allowed for the production of micrometer-sized synthetic polymer fibers. Electrospinning offers substantial prospects for producing nanofillers from polymer solutions. Important

electrospun nanofibers made utilizing a specific solvent[153].

Some studies focused on poly(ethylene terephthalate) (PET). The substrate was chemically treated using ethylenediamine before electrospinning. Three additives were studied: cellulose acetate, polyethylene glycol, and polyethylene oxide. The PET fibers-polymer (nm) composite demonstrated adequate physical qualities, including tensile strength and % at break, compared to other electrospun materials like nylon, which lose strength during electrospinning. The addition of polyethylene glycol or polyethylene oxide in PET solution did not improve fiber strength [154].

Electrospinning technology can manufacture nanofibers from a variety of polymer systems, including high performance, liquid crystalline, polymer blend, and biopolymers[155]. Horrocks et al.'s research of flame retardant textiles discovered that including clay minerals in polymers improved flame retardancy by reducing peak heat release rate [156].

Clay Mineral (nm)-Polypropylene Composite

Manias et al.[157] evaluated the preparation of a composite of Mt and polypropylene (nm). Two types of component materials are identified as effective for creating Mt/propylene nanocomposites:

- Functionalized polypropylene and organo-Mt
- Unmodified (=neat) polypropylene and half-fluoridated organic silic.

The essential circumstances, as well as the properties of polypropylene filaments and tapes incorporating functionalized clay mineral dispersion, were investigated to determine flame retardancy [158]. Clay mineral (nm)-polypropylene composite was created by melting polypropylene in a twinscrew extruder.

Table 3: Clay mineral impacts on filament fibers and fabrics

Composite	Method	Performance effects
Clay mineral (nm) polypropylene	Melt compounding propylene in twin-screw extruder	Increased filament modulus Increased char formation Insignificant effect on flame retardancy
Clay mineral (nm) polypropylene Compatibilizer used was maleic anhydride grafted polypropylene	Melt spinning	Filament produced showed improved tensile strength and thermal stability Enhanced dynamic mechanical properties Creep resistance
Mt-polyurethane (nm) (Mt-PU (nm)) Polyhedral oligomeric silsesquioxanes-polyurethane (nm) (POSS-PU)	Coated on polyester and cotton fabric	Relative to Mt-PU, POSS-PU (nm) coating showed improved flame retardancy
NaMt-branched polyethyleneimine	Coated on cotton fabric	When heated to 500° C, the amount of char produced was 2 orders of magnitude relative to uncoated fabric Reduced afterglow time Reduced total heat release Reduced heat release capacity

Then, polypropylene filament containing clay mineral (nm) was created and tested. The addition of scattered clay mineral enhanced filament modulus. Filament samples demonstrated appropriate textile characteristics for knitting into fabric. Fabric and film samples were tested for burning behavior using limiting oxygen index and cone calorimetry at an external heat flux of 35 kW/m². Although the addition of clay material had no significant effect on flame retardancy, it did promote char formation. The impact of clay mineral (nm) on the physical characteristics of polypropylene was assessed [159].

Melt spinning was used to create composite filaments made of clay mineral (nm) and polypropylene. Maleic anhydride-grafted polypropylene was used as the compatibilizer. Clay mineral (nm) loadings up to 1 wt.% with compatibilizer up to 3 wt.% were

studied. Clay mineral (nm)-polypropylene composite filaments outperformed virgin polypropylene in terms of tensile, thermal, and dynamic mechanical properties, as well as creep resistance, at loadings of 0.25-0.5 wt.% and a compatibilizer/clay mineral ratio of 2:1.

Cellulose Composite

Clay mineral was used to make cellulose composites. Clay mineral-cellulose (nm) composite technology was developed using cellulose from grass, kenaf, cotton fiber, and cotton plant material. The thermal stability of the clay mineral-cellulose (nm) composite has been increased, making it appropriate for end products like nonwovens, papers, and filament fibers [160].

Table 4: Various Application of Clay

composite	Method	Fabric Type	Propeties	Ref
Nanoclay	Coating	Polyester – Cotton – polyester/cotton(50/50)	Improve tensile strength – tear – abrasion resistance	[161]
Nanoclay (Montmorillonite)	Pad – dry - cure	Cotton /nylon	Improve waterproof – fireproof-color, light fistness and Uv of dyed fabric	[162]
Nanoclay(kaolinite)	Coating	Wool	Improve fire retardant	[163]
Poly lactide/clay (montmorillonite) (MMT) nanocomposite	Melt blending	Poly lactide	Improve fire retardant	[164]
Nano Clay/Nano TiO ₂ /Polysiloxane Composites	impregnation-dry-cure	Polyester	Improve self-cleaning, thermal stability and hydrophilic properties	[165]
NanoClay (Montmorillonite)	-	denim fabric (blue jean) 100 % cotton	obtaining washed denim - Desirable handle, air permeability, wrinkle resistance, and abrasion resistance properties	[166]
Nanoclay (Bentonite)	pad - dry - cure technique and IR dyeing machine	Polyester	Improve UV protection - physical and mechanical properties such as tensile strength - elongation% - thickness and moisture regain	[167]
Polyurethane/Clay and Polyurethane/POSS Nanocomposites	Coating	Polyester – Cotton	Improve flame retardant	[149]
polyamide-6/clay hybrid nanocomposite	Melt-spinning	Polyamide 6	Improve flame retardant	[168]
phosphate/clay mineral	Coating	Cotton	Improve flame retardant	[169]
Clay(kaolinite)-TiO ₂ nano-hybrid	incorporating	Cotton	Improve flame retardant	[170]
Nanosilica and nanoclay	Coating	cotton	super-hydrophobic fabric	[171]
Cellulose/nanoclay composite films	pad - dry - cure	cotton	high water vapor resistance	[172]
Nanoclay/ soy flour composite	pad - dry - cure	Jute	Improve flame retardant – physical properites	[173]
Polypropylene/ nanoclay composite	pad - dry - cure	polypropylene	Improve flame retardant	[174]
neat epoxy carpet composite, clay-coated carpet composite, and clay-infused carpet composite	coating	Carpet	Improve flame retardant	[175]
NanoClay (Montmorillonite)	coating	Cotton	Improve flame retardant	[176]

Clay Nanotube-Based Antibacterial Composites

Bone and Tissue Engineering

In recent years, functional materials incorporating halloysite-loaded antibacterial particles or medicines have been created for medical applications, coatings, and polymeric films. Nanofibers produced through electrospinning have been widely explored for tissue engineering and other uses. Drug-loaded fibers are both biocompatible and bactericidal, with delayed drug release due to polymer degradation. Halloysite-polymer composite fibers constructed from polylactic acid, polycaprolactone, poly(caprolactone)/gelatin, and poly(lactic-co-glycolic acid) were tested for antibacterial protection see Figure28.

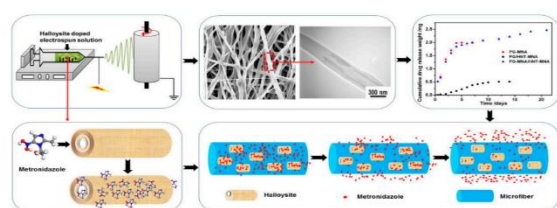


Figure28: Electrospinning drug-loaded halloysite clay nanotubes doped into poly(caprolactone)/gelatin microfiber[177]

Electrospun poly(lactic-co-glycolic acid) nanofibers were treated with halloysite to create a medication delivery system that releases tetracycline hydrochloride slowly. The drug loading efficiency reached 42.65%. Halloysite loading reduces fiber diameter due to the introduction of positively charged tetracycline hydrochloride into the electrospinning liquid. Tetracycline hydrochloride/halloysite/poly(lactic-co-glycolic acid) nanofibrous mats shown good cytocompatibility and antibacterial efficacy, inhibiting bacterial growth in liquid and solid mediums. Nanofibrous mats with drug-loaded halloysite had lower release percentages over 42 days compared to nanofibers with pure drug and tetracycline hydrochloride/halloysite powder on the first day [178].

Electrospinning drug-loaded halloysite clay nanotubes into poly (caprolactone/gelatin) microfibers resulted in the development of guided tissue/bone regeneration membranes with sustained drug delivery [177]. The introduction of 20 wt% nanotubes in fiber membranes enabled 25 wt% metronidazole drug loading in the membrane.

Wound Dressing

Halloysite is useful to create flexible multi-layer wound dressings with adjustable functionality such fluid absorption, antibacterial/fungal protection, and tissue regeneration. The dressing can be used for wound packing, topical gauze, or prophylaxis. Doped clay nanotubes improve dressing properties,

allow for multiple drug loading, and provide better control over drug release kinetics (50+ hours), making them ideal for treating chronic wounds, microbial infections, and multi-vector treatments [179].

Nanoclay coatings have a few innovative uses. They can be utilized to create fibers that facilitate the regulated release of medications, perfumes, or other active ingredients. the integrated species' release. Research efforts using a montmorillonite-nanoclay as a carrier for cosmetic jojoba oil substances have produced nylon fibers that may find usage in skin care products. The goal of these projects is to generate antibacterial fabrics by the controlled release of a biocidal agent. Direct melt compounding was used to incorporate the jojoba oil and nanoclays into the polyamide matrix. This suggests that by adding these materials to a SiO₂ nanosol coating, fibers with controlled releases of various agents (such as medications, essential oils, or insect repellent scents) may be produced. When combined with fire-blocking materials like Nomex, Kevlar, glass fiber, Panox, etc., nanoclay particles can function as extremely high-quality flame-retardant coatings [180].

Reused Waste Water Dyes

The third type of adsorption is coprecipitation, which involves the synthesis of hydrotalcite with certain anions that are integrated into its structure and adsorbed. Dye adsorption via cationic exchange cannot be accomplished in most colors found in nature since they are anionic, which is why hydrotalcite-type clays are used for this recovery [181]. To compensate for the laminar structure of hydrotalcite, anions are inserted, leading to adsorption [182].

High absorbance can be achieved, but further processes are required to get appropriate adsorption characteristics. Gasser, Mekhamer, and Abdel Rahman [183] computed the CEC for this nanoclay to be 8.96 cmol·kg⁻¹. Wastewater is discharged immediately after dyeing activities are completed. This article's findings suggest that a significant amount of dyes can be recovered and reused in industrial operations.

Pigment

One approach for reusing colorants is to use them as pigments[67, 184-186]. Once trapped inside a substrate, like as clay, they can remain there to be used later in stamping processes. To be effective as pigments, colorants must be stable and resistant to desorption. After injecting the colorant into clay, tests are conducted to determine its degree of fixing. High fixing results ensure that the pigment can be used without risk of damage from colorant loss.

These pigments are widely used in industries like textiles, plastics, printing, and industrial coatings, but they have a number of qualities that limit their application, including low stability, poor weather

resistance, and poor dispersion [187, 188]. To ameliorate the abovementioned features and flaws, stabler hybrids with colorants in clay mineral matrices must be created. Hybrids including montmorillonite and methylene blue have been shown to improve thermal stability, photostability, and covering power [189, 190]. Other studies have evaluated the color and stability characteristics of dye-clay hybrids.

According to a 1976 CIELAB investigation [191], halloysite hybrids outperformed other nanoclays like MMT and sepiolite in terms of color stability. This can be due to the unique structure and chemical properties of each nanoclay [192].

Dyes

Another recycling option is to use recovered colorant in another dyeing procedure. To allow for desorption, the clay-dye binding needs to be weaker than in the prior case with a pigment. For this purpose, clays such as Lap are utilized, which, according to testing, have desorption levels ranging from 20% to 40%. Zeolite is another mineral capable of desorbing dyes [10, 193]. According to the bibliographies, desorption techniques involve swirling clay in a bath of distilled water or ethanol. This causes dye desorption [67, 192].

In a work by Momina, Shahadat Mohammad, and Suzylawati Isamil [194], Figure 29 shows how to desorb MB by heating the clay-dye hybrid and utilizing solvents such HCl, ethanol, nitric acid, or acetone. The study found that breaking the connections created during dye adsorption by clay, often known as chemisorption, required more than just heat energy. To regenerate the adsorbent, a thermo-chemical process was necessary due to insufficient energy provided by solvent and heating operations alone.

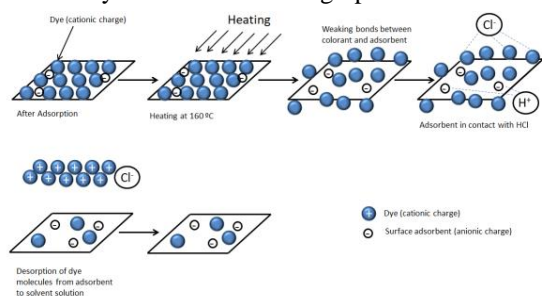


Figure 29: Dye desorption process

The method starts with heating samples to around 150-200 °C for 45 minutes. As a result, the linkages between the adsorbent and colorant weaken. In the next phase, HCl⁻ is used to raise the charges of positive hydrogens, which bind to the clay surface and release Cl⁻ charges that bind to MB. The colorant is then released from the clay, completing the desorption process. Because both elements are ionically neutral, they do not rejoin.

A crucial step in this process is to use thermogravimetric analysis (TGA) to determine the highest temperature that the dye and clay can tolerate. This will raise the initial phase's temperature to a maximum and weaken the binding see Table 4.

Synthes Colorant

Hebeish, A. A., et al [195] Developing a Completely Novel Colorant Hybrid Nanocomposite to Print on a Range of Textile Fabrics (cotton fabrics (100%), cotton/ polyester blend (50/50), wool (100 %), wool/nylon blend (70/30%), wool/polyester blend (45/55%), and acrylic fabric (100 %), Nylon (100 %), viscose/polyester blend (50/50), Natural silk (100 %) and. Polyester (100 %). Clay (MMT) and Indigo Blue Vat dye were combined and heated to 80 °C for 60 minutes to create nanoparticles using an ultrasonic stirrer. Using the created printing pastes, samples of various fabrics were printed both with and without binders. The outcome demonstrated that the color achieved may efficiently function as a pigment color, printing various blends of natural or synthetic fabrics with or without the use of a binder.

Summary

Here is a summary of the key points from the provided text on textile nanotechnology and clay-polymer nanocomposites:

- Clay minerals and clay-polymer nanocomposites are being used in textiles to enhance properties like flame retardancy, mechanical strength, and antibacterial effects.
- Common clay minerals used include montmorillonite, halloysite, and laponite. They are often modified with organic compounds to improve compatibility with polymers.
- Key polymer matrices include polyethylene terephthalate (PET), polypropylene, and cellulose.
- Nanocomposites can be prepared by methods like in-situ polymerization, melt intercalation, and solution blending.
- Benefits of clay nanocomposites in textiles include:
 - Improved mechanical properties
 - Enhanced flame retardancy
 - Better barrier properties
 - Controlled drug/antimicrobial release
 - Improved thermal stability
 - Applications include:
 - Flame retardant fibers and fabrics

Table 5: Reuse Wastewater Dyes

Composite Type	Contaminant Removed	Temp	Adsorption Capacity or Removal Percent	Ref
chitosan–MMT	cationic dye (maxilon blue 5G GR 200%)	RT ^a	99.3%	[196]
chitosan–MMT	anionic dye (lanaset red 2B)	RT ^a	67.4%	[196]
chitosan–MMT	disperse dye (dianix yellow brown SE-R)	RT ^a	68.6%	[196]
chitosan–intercalated MMT	reactive black 5	60	138.89 mg/g	[197]
KSF–MMT–chitosan	reactive blue 19	-	-	[196]
poly(vinyl alcohol)–sodium alginate–chitosan–MMT	methylene blue	30	90%	[198]
chitosan–MMT	reactive red 136	20	74.7%, 445.38 mg/g	[199]
chitosan–halloysite	methylene blue	-	72.60 mg/g	[200]
kaolin–chitosan–titanium dioxide	crystal violet	45	93.30%	[201]
chitosan–bentonite	amaranth red	25	362.1 mg/g	[202]
chitosan–bentonite	methylene blue	25	496.5 mg/g	[202]
chitosan–bentonite	congo red	-	303 mg/g	[203]
N,O-carboxymethylchitosan–MMT	congo red	30-50	-	[204]
magnetic chitosan–MMT	methylene blue	-	82.2 mg/g	[205]
chitosan-grafted poly(acrylamide-itaconic acid)	crystal violet	-	81.6%	[205]
carboxymethyl chitosan–montmorillonite hybrid	congo red	45	84.68 mg/g	[206]
cross-linked chitosan–poly(acrylic acid)–bentonite	malachite green	318 K	454.55 mg/g	[207]
Fe–chitosan–MMT	methylene blue	-	55.81%	[208]
chitosan-activated clay	reactive red 222	30	1912 mg/g	[209]
chitosan- modified kaolinite	basic red 2 orange G	-	37 mg/g 5.99 mg/g	[210]
chitosan–magadiite	congo red methylene blue	30	135.77 mg/g 45.25 mg/g	[211]

- Antibacterial wound dressings
- Controlled release fibers for cosmetics/pharmaceuticals
- Bone and tissue engineering scaffolds
- Clay nanotubes like halloysite are being explored for drug delivery in electrospun fibers.
- Clays are also being investigated to adsorb and recycle dyes from textile wastewater.

The text provides a comprehensive overview of the current research and applications of clay-based nanocomposites in the textile industry, highlighting their potential to impart multifunctional properties to fibers and fabrics.

Conflict of Interest

There is no conflict of interest in the publication of this article.

Acknowledgment

The authors thank the National Research Centre, Giza, Egypt for the financial support of this work and

are also gratefully grateful to the Faculty of Applied Arts, Benha University

Funds

There is no funding

References

1. Lite, M.C., Tănăsescu, E.C., Secăreanu, L.O., Săndulache, I.M., Iordache, O. and Perdum, E. Review on different types of clay and their use as antimicrobial agents for textiles treatment, *TEXTEH Proceedings*, **2021** 321-327 (2021).
2. Galpaya, D., Wang, M., Liu, M., Motta, N., Waclawik, E. and Yan, C. Recent advances in fabrication and characterization of graphene-polymer nanocomposites, *Graphene*, **01**(02) 30-49 (2012).
3. Yeh, M.-H. and Hwang, W.-S. High mechanical properties of polychloroprene/montmorillonite nanocomposites, *Materials Transactions*, **47**(11) 2753-2758 (2006).
4. Hassabo, A.G., Shaarawy, S., Mohamed, A.L. and Hebesh, A. Multifarious cellulosic through

- innovation of highly sustainable composites based on moringa and other natural precursors, *International Journal of Biological Macromolecules*, **165** 141-155 (2020).
5. Hassabo, A.G., Mohamed, A.L., Shaarawy, S. and Hebeish, A. Novel micro-composites based on phosphorylated biopolymer/polyethyleneimine/clay mixture for cotton multi-functionalities performance, *Bioscience Research*, **15**(3) 2568-2582 (2018).
 6. Lo'pez-Manchado, M.A., Arroyo, M., Herrero, B. and Biagiotti, J. Vulcanization kinetics of natural rubber-organoclay nanocomposites, *Journal of Applied Polymer Science*, **89**(1) 1-15 (2003).
 7. Thomas, S., R. Stephen, R.N.P., properties and Sons., a.a.J.W. Rubber nanocomposites: Preparation, properties and application. 2010: John wiley & sons.
 8. Hou, D., Zhang, G., Pant, R.R., Wei, Z. and Shen, S. Micromechanical properties of nanostructured clay-oxide multilayers synthesized by layer-by-layer self-assembly, *Nanomaterials (Basel)*, **6**(11) (2016).
 9. Ant'nez-Garc'ia, J., Galv'an, D.H., Petranovskii, V., Murrieta-Rico, F.N., Yocupicio-Gaxiola, R.I., Shelyapina, M.G. and Fuentes-Moyado, S. The effect of chemical composition on the properties of lta zeolite: A theoretical study, *Computational Materials Science*, **196** (2021).
 10. Mittal, H., Babu, R., Dabbawala, A.A., Stephen, S. and Alhassan, S.M. Zeolite-y incorporated karaya gum hydrogel composites for highly effective removal of cationic dyes, *Colloids and Surfaces A: Physicochemical and Engineering Aspects*, **586** (2020).
 11. Si, D., Zhu, M., Sun, X., Xue, M., Li, Y., Wu, T., Gui, T., Kumakiri, I., Chen, X. and Kita, H. Formation process and pervaporation of high aluminum zsm-5 zeolite membrane with fluoride-containing and organic template-free gel, *Separation and Purification Technology*, **257** (2021).
 12. Lo, A.-Y. and Taghipour, F. Review and prospects of microporous zeolite catalysts for co2 photoreduction, *Applied Materials Today*, **23** (2021).
 13. Wang, C., Cao, L. and Huang, J. Influences of acid and heat treatments on the structure and water vapor adsorption property of natural zeolite, *Surface and Interface Analysis*, **49**(12) 1249-1255 (2017).
 14. Probst, J., Outram, J.G., Couperthwaite, S.J., Millar, G.J. and Kaparaju, P. Sustainable ammonium recovery from wastewater: Improved synthesis and performance of zeolite n made from kaolin, *Microporous and Mesoporous Materials*, **316** (2021).
 15. Misaelides, P. Application of natural zeolites in environmental remediation: A short review, *Microporous and Mesoporous Materials*, **144**(1-3) 15-18 (2011).
 16. Zhao, Z. and Wang, X. Application of anmbr ion exchange technology in water treatment, *IOP Conference Series: Earth and Environmental Science*, **791**(1) (2021).
 17. Breck, D.W. Zeolite molecular sieves: Structure, chemistry and use; krieger; john wiley & sons: New york, ny, USA, 1984.
 18. Wajima, T., Yoshizuka, K., Hirai, T. and Ikegami, Y. Synthesis of zeolite x from waste sandstone cake using alkali fusion method, *Materials Transactions*, **49**(3) 612-618 (2008).
 19. Shoppert, A.A., Loginova, I.V., Chaikin, L.I. and Rogozhnikov, D.A. Alkali fusion-leaching method for comprehensive processing of fly ash, *KnE Materials Science*, **2**(2) (2017).
 20. Tsujiguchi, M., Kobashi, T., Oki, M., Utsumi, Y., Kakimori, N. and Nakahira, A. Synthesis and characterization of zeolite a from crushed particles of aluminoborosilicate glass used in lcd panels, *Journal of Asian Ceramic Societies*, **2**(1) 27-32 (2018).
 21. PEROT, G. and GUIUNET, M. Advantages and disadvantages of zeolites as catalysts in organic chemistry, *Journal of Molecular Catalysis*, **61** 173-196 (1990).
 22. Parades-Aguilar, J., Reyes-Martinez, V., Bustamante, G., Almendariz-Tapia, F.J., Martinez-Meza, G., Vilchez-Vargas, R., Link, A., Certucha-Barragan, M.T. and Calderon, K. Removal of nickel(ii) from wastewater using a zeolite-packed anaerobic bioreactor: Bacterial diversity and community structure shifts, *J Environ Manage*, **279** 111558 (2021).
 23. Saqib, N.U., Adnan, R., Rahim, M. and Khan, A. Low-cost zeolite/TiO2 composite for the photocatalytically enhanced adsorption of cd2+ from aqueous solution, *Journal of the Iranian Chemical Society*, **18**(8) 2165-2180 (2021).
 24. Liu, M., Jia, Z., Jia, D. and Zhou, C. Recent advance in research on halloysite nanotubes-polymer nanocomposite, *Progress in Polymer Science*, **39**(8) 1498-1525 (2014).
 25. Lazaratou, C.V., Panagiotaras, D., Panagopoulos, G., Posp'isil, M. and Papoulis, D. Ca treated palygorskite and halloysite clay minerals for ferrous iron (fe+2) removal from water systems, *Environmental Technology & Innovation*, **19** (2020).
 26. Van Ranst, E., Kips, P., Mbogoni, J., Mees, F., Dumon, M. and Delvaux, B. Halloysite-smectite

- mixed-layered clay in fluvio-volcanic soils at the southern foot of mount kilimanjaro, tanzania, *Geoderma*, **375** (2020).
27. Zhao, N., Liu, Y., Zhao, X. and Song, H. Liquid crystal self-assembly of halloysite nanotubes in ionic liquids: A novel soft nanocomposite ionogel electrolyte with high anisotropic ionic conductivity and thermal stability, *Nanoscale*, **8**(3) 1545-54 (2016).
 28. Lazzara, G., Cavallaro, G., Panchal, A., Fakhruddin, R., Stavitskaya, A., Vinokurov, V. and Lvov, Y. An assembly of organic-inorganic composites using halloysite clay nanotubes, *Current Opinion in Colloid & Interface Science*, **35** 42-50 (2018).
 29. Yendluri, R., Otto, D.P., De Villiers, M.M., Vinokurov, V. and Lvov, Y.M. Application of halloysite clay nanotubes as a pharmaceutical excipient, *Int J Pharm*, **521**(1-2) 267-273 (2017).
 30. Yuan, P., Tan, D. and Annabi-Bergaya, F. Properties and applications of halloysite nanotubes: Recent research advances and future prospects, *Applied Clay Science*, **112-113** 75-93 (2015).
 31. Pasbakhsh, P., Churchman, G.J. and Keeling, J.L. Characterisation of properties of various halloysites relevant to their use as nanotubes and microfibre fillers, *Applied Clay Science*, **74** 47-57 (2013).
 32. Li, R., Yang, J., Hu, J., Zhang, G. and Zhu, P. Effects of various decolorizing agents on waste cotton fabric dyed with reactive dyes, *research square*, 1-23 (2021).
 33. Liu, W., Fizir, M., Hu, F., Li, A., Hui, X., Zha, J. and He, H. Mixed hemimicelle solid-phase extraction based on magnetic halloysite nanotubes and ionic liquids for the determination and extraction of azo dyes in environmental water samples, *J Chromatogr A*, **1551** 10-20 (2018).
 34. Zhao, M. and Liu, P. Adsorption behavior of methylene blue on halloysite nanotubes, *Microporous and Mesoporous Materials*, **112**(1-3) 419-424 (2008).
 35. Luo, P., Zhang, B., Zhao, Y., Wang, J., Zhang, H. and Liu, J. Removal of methylene blue from aqueous solutions by adsorption onto chemically activated halloysite nanotubes, *Korean Journal of Chemical Engineering*, **28**(3) 800-807 (2011).
 36. Liu, Y., Zheng, Y. and Wang, A. Response surface methodology for optimizing adsorption process parameters for methylene blue removal by a hydrogel composite, *Adsorption Science & Technology*, **28** 913-922 (2010).
 37. Liu, L., Wan, Y., Xie, Y., Zhai, R., Zhang, B. and Liu, J. The removal of dye from aqueous solution using alginate-halloysite nanotube beads, *Chemical Engineering Journal*, **187** 210-216 (2012).
 38. Jiang, L., Zhang, C., Wei, J., Tjiu, W., Pan, J., Chen, Y. and Liu, T. Surface modifications of halloysite nanotubes with superparamagnetic fe₃o₄ nanoparticles and carbonaceous layers for efficient adsorption of dyes in water treatment, *Chemical Research in Chinese Universities*, **30**(6) 971-977 (2014).
 39. Nguyen, T.K.L., Cao, X.T., Park, C. and Lim, K.T. Preparation, characterization and application of magnetic halloysite nanotubes for dye removal, *Molecular Crystals and Liquid Crystals*, **644**(1) 153-159 (2017).
 40. Wan, X., Zhan, Y., Long, Z., Zeng, G. and He, Y. Core@double-shell structured magnetic halloysite nanotube nano-hybrid as efficient recyclable adsorbent for methylene blue removal, *Chemical Engineering Journal*, **330** 491-504 (2017).
 41. Farrokhi-Rad, M., Mohammadalipour, M. and Shahrabi, T. Electrophoretically deposited halloysite nanotubes coating as the adsorbent for the removal of methylene blue from aqueous solution, *Journal of the European Ceramic Society*, **38**(10) 3650-3659 (2018).
 42. Liu, R., Fu, K., Zhang, B., Mei, D., Zhang, H. and Liu, J. Removal of methyl orange by modified halloysite nanotubes, *Journal of Dispersion Science and Technology*, **33**(5) 711-718 (2012).
 43. Chen, H., Zhao, J., Wu, J. and Yan, H. Selective desorption characteristics of halloysite nanotubes for anionic azo dyes, *RSC Advances*, **4**(30) (2014).
 44. Shahamati Fard, F., Akbari, S., Pajootan, E. and Arami, M. Enhanced acidic dye adsorption onto the dendrimer-based modified halloysite nanotubes, *Desalination and Water Treatment*, **57**(54) 26222-26239 (2016).
 45. Zango, Z.U., Abu Bakar, N.H.H., Tan, W.L. and Bakar, M.A. Enhanced removal efficiency of methyl red via the modification of halloysite nanotubes by copper oxide, *Journal of Dispersion Science and Technology*, **39**(1) 148-154 (2017).
 46. Cavallaro, G., Gianguzza, A., Lazzara, G., Milioto, S. and Piazzese, D. Alginate gel beads filled with halloysite nanotubes, *Applied Clay Science*, **72** 132-137 (2013).
 47. Kiani, G., Dostali, M., Rostami, A. and Khataee, A.R. Adsorption studies on the removal of malachite green from aqueous solutions onto halloysite nanotubes, *Applied Clay Science*, (2011).
 48. Bessaha, F., Marouf-Khelifa, K., Batonneau-Gener, I. and Khelifa, A. Characterization and application of heat-treated and acid-leached halloysites in the removal of malachite green: Adsorption, desorption, and regeneration studies, *Desalination and Water Treatment*, **57**(31) 14609-14621 (2015).

49. Duan, J., Liu, R., Chen, T., Zhang, B. and Liu, J. Halloysite nanotube- Fe_3O_4 composite for removal of methyl violet from aqueous solutions, *Desalination*, **293** 46-52 (2012).
50. Bonetto, L.R., Ferrarini, F., de Marco, C., Crespo, J.S., Guégan, R. and Giovanela, M. Removal of methyl violet 2b dye from aqueous solution using a magnetic composite as an adsorbent, *Journal of Water Process Engineering*, **6** 11-20 (2015).
51. Mudhoo, A., Gautam, R.K., Ncibi, M.C., Zhao, F., Garg, V.K. and Sillanpää, M. Green synthesis, activation and functionalization of adsorbents for dye sequestration, *Environmental Chemistry Letters*, **17**(1) 157-193 (2018).
52. Riahi-Madvaar, R., Taher, M.A. and Fazilrad, H. Synthesis and characterization of magnetic halloysite-iron oxide nanocomposite and its application for naphthol green b removal, *Applied Clay Science*, **137** 101-106 (2017).
53. Massaro, M., Colletti, C.G., Lazzara, G., Guernelli, S., Noto, R. and Riela, S. Synthesis and characterization of halloysite-cyclodextrin nanosponges for enhanced dyes adsorption, *ACS Sustainable Chemistry & Engineering*, **5**(4) 3346-3352 (2017).
54. Zhao, Y., Abdullayev, E., Vasiliev, A. and Lvov, Y. Halloysite nanotubule clay for efficient water purification, *J Colloid Interface Sci*, **406** 121-9 (2013).
55. Jinhua, W., Xiang, Z., Bing, Z., Yafei, Z., Rui, Z., Jindun, L. and Rongfeng, C. Rapid adsorption of Cr(VI) on modified halloysite nanotubes, *Desalination*, **259**(1-3) 22-28 (2010).
56. Al-Beladi, A.A., Kosa, S.A., Abdul Wahab, R. and Salam, M.A. Removal of orange G dye from real water using halloysite nanoclay-supported ZnO nanoparticles, *Desalination and Water Treatment*, **196** 287-298 (2020).
57. Sprynskyy, M., Sokol, H., Rafinska, K., Brzozowska, W., Railean-Plugaru, V., Pomastowski, P. and Buszewski, B. Preparation of agnps/saponite nanocomposites without reduction agents and study of its antibacterial activity, *Colloids Surf B Biointerfaces*, **180** 457-465 (2019).
58. Lima, L.C.B., Silva, F.C., Silva-Filho, E.C., Fonseca, M.G., Zhuang, G. and Jaber, M. Saponite-anthocyanin derivatives: The role of organoclays in pigment photostability, *Applied Clay Science*, **191** (2020).
59. Brandão Lima, L.C., Castro-Silva, F., Silva-Filho, E.C., Fonseca, M.G. and Jaber, M. Saponite-anthocyanin pigments: Slipping between the sheets, *Microporous and Mesoporous Materials*, **300** (2020).
60. Fatimah, I., Nurillahi, R., Sahroni, I. and Muraza, O. TiO_2 -pillared saponite and photosensitization using a ruthenium complex for photocatalytic enhancement of the photodegradation of bromophenol blue, *Applied Clay Science*, **183** (2019).
61. Kenne Dedzo, G., Rigolet, S., Josien, L., Ngameni, E. and Dzene, L. Functionalization of synthetic saponite: Identification of grafting sites and application for anions sequestration, *Applied Surface Science*, **567** (2021).
62. Casagrande, M., Storaro, L., Lenarda, M. and Rossini, S. Solid acid catalysts from clays: Oligomerization of 1-pentene on Al-pillared smectites, *Catalysis Communications*, **6**(8) 568-572 (2005).
63. Takagi, S., Shimada, T., Ishida, Y., Fujimura, T., Masui, D., Tachibana, H., Eguchi, M. and Inoue, H. Size-matching effect on inorganic nanosheets: Control of distance, alignment, and orientation of molecular adsorption as a bottom-up methodology for nanomaterials, *Langmuir*, **29**(7) 2108-19 (2013).
64. Utracki, L.A., Sepehr, M. and Boccaleri, E. Synthetic, layered nanoparticles for polymeric nanocomposites (pncs), *Polymers for Advanced Technologies*, **18**(1) 1-37 (2007).
65. Franco, F., Benítez-Guerrero, M., Gonzalez-Triviño, I., Pérez-Recuerda, R., Assiego, C., Cifuentes-Melchor, J. and Pascual-Cosp, J. Low-cost aluminum and iron oxides supported on dioctahedral and trioctahedral smectites: A comparative study of the effectiveness on the heavy metal adsorption from water, *Applied Clay Science*, **119** 321-332 (2016).
66. Ragu, S., Dardillac, E., Brooks, D.A., CastroSmirnov, F.A., Aranda, P., Ruiz-Hitzky, E. and Lope, B.S. Responses of human cells to sepiolite interaction, *Applied Clay Science*, **194** (2020).
67. Chen, H., Zhang, Z., Zhuang, G. and Jiang, R. A new method to prepare 'maya red' pigment from sepiolite and basic red 46, *Applied Clay Science*, **174** 38-46 (2019).
68. Galan, E. Properties and applications of palygorskite-sepiolite clays, *Clay Minerals*, **31**(4) 443-453 (2018).
69. Hamid, Y., Tang, L., Hussain, B., Usman, M., Liu, L., Ulhassan, Z., He, Z. and Yang, X. Sepiolite clay: A review of its applications to immobilize toxic metals in contaminated soils and its implications in soil-plant system, *Environmental Technology & Innovation*, **23** (2021).
70. Santos, S.C.R. and Boaventura, R.A.R. Adsorption of cationic and anionic azo dyes on sepiolite clay: Equilibrium and kinetic studies in batch mode, *Journal of Environmental Chemical Engineering*, **4**(2) 1473-1483 (2016).

71. Cheng, H., Zhu, Q. and Xing, Z. Adsorption of ammonia nitrogen in low temperature domestic wastewater by modification bentonite, *Journal of Cleaner Production*, **233** 720-730 (2019).
72. Miz, M.E., Akichoh, H., Berraouan, D., Salhi, S. and Tahani, A. Chemical and physical characterization of moroccan bentonite taken from nador (north of morocco), *American Journal of Chemistry*, **7**(4) 105-112 (2017).
73. Angar, Y., Djelali, N.E. and Kebbouche-Gana, S. Investigation of ammonium adsorption on algerian natural bentonite, *Environ Sci Pollut Res Int*, **24**(12) 11078-11089 (2017).
74. Ghadiri, M., Hau, H., Chrzanowski, W., Agus, H. and Rohanzadeh, R. Laponite clay as a carrier for in situ delivery of tetracycline, *RSC Advances*, **3**(43) (2013).
75. Bienia, M., Danglade, C., Lecomte, A., Brevier, J. and Pagnoux, C. Cylindrical couette flow of laponite dispersions, *Applied Clay Science*, **162** 83-89 (2018).
76. Loginov, M., Lebovka, N. and Vorobiev, E. Laponite assisted dispersion of carbon nanotubes in water, *J Colloid Interface Sci*, **365**(1) 127-36 (2012).
77. Manilo, M.V., Lebovka, N. and Barany, S. Combined effect of cetyltrimethylammonium bromide and laponite platelets on colloidal stability of carbon nanotubes in aqueous suspensions, *Journal of Molecular Liquids*, **235** 104-110 (2017).
78. Le Coeur, C., Lorthioir, C., Feoktystov, A., Wu, B., Volet, G. and Amiel, C. Laponite/poly(2-methyl-2-oxazoline) hydrogels: Interplay between local structure and rheological behaviour, *J Colloid Interface Sci*, **582**(Pt A) 149-158 (2021).
79. Zhang, R., Xie, L., Wu, H., Yang, T., Zhang, Q., Tian, Y., Liu, Y., Han, X., Guo, W., He, M., Liu, S. and Tian, W. Alginate/laponite hydrogel microspheres co-encapsulating dental pulp stem cells and vegf for endodontic regeneration, *Acta Biomater*, **113** 305-316 (2020).
80. Au, P.-I., Hassan, S., Liu, J. and Leong, Y.-K. Behaviour of laponite® gels: Rheology, ageing, pH effect and phase state in the presence of dispersant, *Chemical Engineering Research and Design*, **101** 65-73 (2015).
81. Valencia, G.A., Djabourov, M., Carn, F. and Sobral, P.J.A. Novel insights on swelling and dehydration of laponite, *Colloid and Interface Science Communications*, **23** 1-5 (2018).
82. Zhang, P., Wang, J., Jia, Y., Li, W., Tan, X., Zhang, D., Xu, S., Zhang, P., Wei, C. and Miao, S. Encapsulating spinel nanocrystals in laponite cages and applications in molecular oxidation of cyclohexane, *Applied Clay Science*, **181** (2019).
83. Takeno, H. and Sato, C. Effects of molecular mass of polymer and composition on the compressive properties of hydrogels composed of laponite and sodium polyacrylate, *Applied Clay Science*, **123** 141-147 (2016).
84. Taguchi, T., Kohno, Y., Shibata, M., Tomita, Y., Fukuhara, C. and Maeda, Y. An easy and effective method for the intercalation of hydrophobic natural dye into organo-montmorillonite for improved photostability, *Journal of Physics and Chemistry of Solids*, **116** 168-173 (2018).
85. Kohno, Y., Senga, M., Shibata, M., Yoda, K., Matsushima, R., Tomita, Y., Maeda, Y. and Kobayashi, K. Stabilization of flavylum dye by incorporation into fe-containing mesoporous silicate, *Microporous and Mesoporous Materials*, **141**(1-3) 77-80 (2011).
86. Kohno, Y., Asai, S., Shibata, M., Fukuhara, C., Maeda, Y., Tomita, Y. and Kobayashi, K. Improved photostability of hydrophobic natural dye incorporated in organo-modified hydrotalcite, *Journal of Physics and Chemistry of Solids*, **75**(8) 945-950 (2014).
87. Akil, J., Ciotonea, C., Siffert, S., Royer, S., Pirault-Roy, L., Cousin, R. and Poupin, C. No reduction by co under oxidative conditions over cocual mixed oxides derived from hydrotalcite-like compounds: Effect of water, *Catalysis Today*, **384-386** 97-105 (2022).
88. Adsorption of anionic species on hydrotalcite-like compounds: Effect of interlayer anion and crystallinity, *Applied Clay Science* **18** 17-27 (2001).
89. Hassani, I.E.A.E. and Sadik, C. Geology and mineralogy of clays for nanocomposites: State of knowledge and methodology, *Engineering Materials*, 85-114.
90. Michard, A. Eléments de géologie marocaine, notes et mem. Serv. Géol. Maroc, n° 252, pp. 408 (1976).
91. Bhattacharji, S., Neugebauer, B.H.J., Reitner, B.J. and Göttingen K. Stüwe, G. Continental evolution: The geology of morocco. Structure, stratigraphy, and tectonics of the africa-atlantic-mediterranean triple junction, *Edition Springer*, 404 (2008).
92. Seghar, S., Ait Hocine, N., Mittal, V., Azem, S., Al-Zohbi, F., Schmaltz, B. and Poirot, N. Devulcanization of styrene butadiene rubber by microwave energy: Effect of the presence of ionic liquid, *Express Polymer Letters*, **9**(12) 1076-1086 (2015).
93. Obaje, S.O., Omada, J.I. and Dambatta, U.A. Clays and their industrial applications: Synoptic review, *International Journal of Science and Technology*, **5** 264-265 (2013).

94. Bergaya, F. and Lagaly, G. General introduction: Clays, clay minerals, and clay science, 2nd edn. Elsevier Ltd (2013).
95. Yui, T., Fujii, S., Matsubara, K., Sasai, R., Tachibana, H., Yoshida, H., Takagi, K. and Inoue, H. Intercalation of a surfactant with a long polyfluoroalkyl chain into a clay mineral: Unique orientation of polyfluoroalkyl groups in clay layers, *Langmuir*, **29**(34) 10705-12 (2013).
96. Weissenbach, K. and Mack, H. Functional fillers for plastics. In: Silane coupling agents, in functional fillers for plastics, pp 57–83. Wiley-vch verlag gmbh & co. Kga (2005).
97. Matinlinna, J.P., Choi, A.H. and Tsoi, J.K. Bonding promotion of resin composite to silica-coated zirconia implant surface using a novel silane system, *Clin Oral Implants Res*, **24**(3) 290-6 (2013).
98. Avila, L.R., de Faria, E.H., Ciuffi, K.J., Nassar, E.J., Calefi, P.S., Vicente, M.A. and Trujillano, R. New synthesis strategies for effective functionalization of kaolinite and saponite with silylating agents, *J Colloid Interface Sci*, **341**(1) 186-93 (2010).
99. Alkan, M., Hopa, Ç., Yilmaz, Z. and Güler, H. The effect of alkali concentration and solid/liquid ratio on the hydrothermal synthesis of zeolite naa from natural kaolinite, *Microporous and Mesoporous Materials*, **86**(1-3) 176-184 (2005).
100. Sanchez-Fernandez, A., Pena-Paras, L., Vidaltamayo, R., Cue-Sampedro, R., Mendoza-Martinez, A., Zomosa-Signoret, V.C., Rivas-Estilla, A.M. and Riojas, P. Synthesis, characterization, and in vitro evaluation of cytotoxicity of biomaterials based on halloysite nanotubes, *Materials (Basel)*, **7**(12) 7770-7780 (2014).
101. Jeong, E., Lim, J.W., Seo, K.-w. and Lee, Y.-S. Effects of physicochemical treatments of illite on the thermo-mechanical properties and thermal stability of illite/epoxy composites, *Journal of Industrial and Engineering Chemistry*, **17**(1) 77-82 (2011).
102. Navrátilová, Z., Wojtowicz, P., Vaculíková, L. and Sugarkova, V. Sorption of alkylammonium cations on montmorillonite, *Acta Geodynamica et Geomaterialia*, **4** 59–65 (2007).
103. Kotal, M. and Bhowmick, A.K. Polymer nanocomposites from modified clays: Recent advances and challenges, *Progress in Polymer Science*, **51** 127-187 (2015).
104. Nguyen, Q.T. and Baird, D.G. Preparation of polymer–clay nanocomposites and their properties, *Advances in Polymer Technology*, **25**(4) 270-285 (2007).
105. Hussain, F., Hojjati, M., Okamoto, M. and Gorga, R.E. Review article: Polymer-matrix nanocomposites, processing, manufacturing, and application: An overview, *Journal of Composite Materials*, **40**(17) 1511-1575 (2006).
106. Santos, S.C.R. and Boaventura, R.A.R. Adsorption modelling of textile dyes by sepiolite, *Applied Clay Science*, **42**(1-2) 137-145 (2008).
107. Shanmugaraj, A.M., Rhee, K.Y. and Ryu, S.H. Influence of dispersing medium on grafting of aminopropyltriethoxysilane in swelling clay materials, *J Colloid Interface Sci*, **298**(2) 854-9 (2006).
108. Ha, S.R., Ryu, S.H., Park, S.J. and Rhee, K.Y. Effect of clay surface modification and concentration on the tensile performance of clay/epoxy nanocomposites, *Materials Science and Engineering: A*, **448**(1-2) 264-268 (2007).
109. Park, M., Shim, I.-K., Jung, E.-Y. and Choy, J.-H. Modification of external surface of laponite by silane grafting, *Journal of Physics and Chemistry of Solids*, **65**(2-3) 499-501 (2004).
110. Chen, G.X. and Yoon, J.S. Clay functionalization and organization for delamination of the silicate tactoids in poly(l-lactide) matrix, *Macromolecular Rapid Communications*, **26**(11) 899-904 (2005).
111. Wypych, F. Chemical modification of clay surfaces in encyclopaedia of surface and colloid science. 2006, taylor & francis. P. 1256-1272.
112. de Paiva, L.B., Morales, A.R. and Valenzuela Díaz, F.R. Organoclays: Properties, preparation and applications, *Applied Clay Science*, **42**(1-2) 8-24 (2008).
113. S.S. B. and Aadhar, M. Studies on preparation and analysis of organoclay nano particles, *Research Journal of Engineering Sciences*, **3**(3) 10-16 (2014).
114. Olphen, H.v. An introduction to clay colloid chemistry, John Wiley & Sons., New York: Interscience Publishers., pp. 230-230. , (1964).
115. Morgan, A.B. and Wilkie, C.A. Practical issues and future trends in polymer nanocomposite flammability research, 355-399 (2007).
116. Jang, B.N., D. Wang and Wilkie, C.A. Relationship between the solubility parameter of polymers and the clay dispersion in polymer/clay nanocomposites and the role of the surfactant, *Macromolecules*, **38**(15) 6533-6543 (2005).
117. Murray, H.H. Traditional and new applications for kaolin, smectite, and palygorskite: A general overview, *Applied Clay Science*, **17**(5) 207-221 (2000).
118. Ogawa, M. and Kuroda, K. Preparation of inorganic–organic nanocomposites through intercalation of organoammonium ions into layered silicates,

- Bulletin of the Chemical Society of Japan*, **70**(11) 2593-2618 (1997).
119. Gilman, J.W., Awad, W.H., Davis, R.D., Shields, J., Harris, R.H., Davis, C., Morgan, A.B., Sutto, T.E., Callahan, J., Trulove, P.C. and DeLong, H.C. Polymer/layered silicate nanocomposites from thermally stable trialkylimidazolium-treated montmorillonite, *Chemistry of Materials*, **14**(9) 3776-3785 (2002).
120. Douglas A. Brune and Bicerano, J. Micromechanics of nanocomposites: Comparison of tensile and compressive elastic moduli, and prediction of effects of incomplete exfoliation and imperfect alignment on modulus, *Polymer* **43** 369-387 (2002).
121. Bharadwaj, R.K. Modeling the barrier properties of polymer-layered silicate nanocomposites, *Macromolecules*, **34** 9189-9192 (2001).
122. Gilman, J.W., et al. Flammability properties of polymer-layered-silicate nanocomposites. Polypropylene and polystyrene nanocomposites, *Chemistry of Materials* **12**(7) 1866-1873 (2000).
123. Zhu, J., Morgan, A.B., Lamelas, F.K. and Wilkie, C.A. Fire properties of polystyrene-clay nanocomposites, *Chemistry of Materials*, **13**(10) 3774-3780 (2001).
124. Ishida, H., S. Campbell and Blackwell, J. General approach to nanocomposite preparation, *Chemistry of Materials*, **12**(5) 1260-1267 (2000).
125. Yoonessi, M., Toghiani, H., Kingery, W.L. and Pittman, C.U. Preparation, characterization, and properties of exfoliated/delaminated organically modified clay/dicyclopentadiene resin nanocomposites, *Macromolecules* **37** 2511-2518 (2004).
126. Morgan, A.B., Gilman, J.W. and C.L. Jackson Proceedings of the american chemical society: Polymeric materials science & engineering. 2000, washington, dc, san francisco, ca.
127. Morgan, A.B. and Gilman, J.W. Characterization of polymer-layered silicate (clay) nanocomposites by transmission electron microscopy and x-ray diffraction: A comparative study, *Journal of Applied Polymer Science*, **87**(8) 1329-1338 (2003).
128. Kashiwagi, T., Grulke, E., Hilding, J., Harris, R., Awad, W. and Douglas, J. Thermal degradation and flammability properties of poly(propylene)/carbon nanotube composites, *Macromolecular Rapid Communications*, **23**(13) 761-765 (2002).
129. Kojima, Y., et al One-pot synthesis of nylon 6-clay hybrid, **31**(7) 1755-1758 (1993).
130. Morgan, A.B., Chu, L.-L. and Harris, J.D. A flammability performance comparison between synthetic and natural clays in polystyrene nanocomposites, *Fire and Materials*, **29**(4) 213-229 (2005).
131. Xie, W., et al Thermal stability of quaternary phosphonium modified montmorillonites, *Chemistry of Materials*, **14**(11) 4837-4845 (2002).
132. Carrado, K.A. Synthetic organo- and polymer-clays: Preparation, characterization, and materials applications, *Applied Clay Science*, **17**(1) 1-23 (2000).
133. Beyer, G. Nanocomposites: A new class of flame retardants for polymers, **4** 22-28 (2002).
134. Su, S., Jiang, D.D. and Wilkie, C.A. Poly(methyl methacrylate), polypropylene and polyethylene nanocomposite formation by melt blending using novel polymerically-modified clays, **83** 321-331 (2004).
135. Vaia, R.A. and Giannelis, E.P. Lattice model of polymer melt intercalation in organically-modified layered silicates, *Macromolecules*, **30** 7990-7999 (1997).
136. Zhao, X., Urano, K. and Ogasawara, S. Adsorption of polyethylene glycol from aqueous solution on montmorillonite clays, *Colloid and Polymer Science*, **267** 899-906 (1989).
137. Jeon, H.G., Jung, H.-T., Lee, S.W. and Hudson, S.D. Morphology of polymer/silicate nanocomposites, *Polymer Bulletin*, **41** 107-113 (1998).
138. Sur, G.S., Sun, H.L., Lyu, S.G. and Mark, J.E. Synthesis, structure, mechanical properties, and thermal stability of some polysulfone/organoclay nanocomposites, *Polymer* **42** 9783-9789 (2001).
139. Usuki, A., Kawasumi, M., Kojima, Y., Okada, A., Kurauchi, T. and Kamigaito, O. Swelling behavior of montmorillonite cation exchanged for v-amino acids by epsilon-caprolactam, *Journal of Materials Research*, 1174-1184 (1993).
140. Zanetti, M., Lomakin, S. and Camino, G. Polymer layered silicate nanocomposites, *Macromolecular Materials and Engineering*, **279**(1) 1-9 (2000).
141. Bergman, J.S., Chen, H., Giannelis, E.P., Thomas, M.G. and Coates, G.W. Synthesis and characterization of polyolefin-silicate nanocomposites: A catalyst intercalation and in situ polymerization approach, *Chemical Communications*, **21** 2179-2180 (1999).
142. Vaia, R.A., Ishii, H. and Giannelis, E.P. Synthesis and properties of two-dimensional nanostructures by direct intercalation of polymer melts in layered silicates, *Chemistry of Materials* **5**(12) 1694-1696 (1993).
143. Liu, L., Qi, Z. and Zhu, X. Studies on nylon 6/clay nanocomposites by melt-intercalation process,

- Journal of Applied Polymer Science*, **71**(7) 1133-1138 (1999).
144. Timmaraju, M.V., Gnanamoorthy, R. and Kannan, K. Influence of imbibed moisture and organoclay on tensile and indentation behavior of polyamide 66/hectorite nanocomposites, *Composites Part B: Engineering*, **42**(3) 466-472 (2011).
145. Ferreira, J.A.M., Reis, P.N.B., Costa, J.D.M., Richardson, B.C.H. and Richardson, M.O.W. A study of the mechanical properties on polypropylene enhanced by surface treated nanoclays, *Composites Part B: Engineering*, **42**(6) 1366-1372 (2011).
146. Jose-Yacaman, M., et al and 223-5., p. Maya blue paint: An ancient nanostructured material, *Science*, **273**(5272) 223-225 (1996).
147. Uddin, F. Some aspects in textile nanofinishing,” in proceedings the 86th textile institute world conference, the hong kong polytechnic university, november 2008.
148. Dastjerdi, R. and Montazer, M. A review on the application of inorganic nano-structured materials in the modification of textiles: Focus on anti-microbial properties, *Colloids Surf B Biointerfaces*, **79**(1) 5-18 (2010).
149. Devaux, E., Rochery, M. and Bourbigot, S. Polyurethane/clay and polyurethane/poss nanocomposites as flame retarded coating for polyester and cotton fabrics, *Fire and Materials*, **26**(4-5) 149-154 (2002).
150. Li, Y.-C., Schulz, J., Zammarano, M., Mannen, S., Grunlan, J.C., Delhom, C., Condon, B. and Chang, S. Flame retardant behavior of polyelectrolyte-clay thin film assemblies on cotton fabric, *ACS Nano*, **4**(6) 3325-3337 (2010).
151. Almecija, D., Blond, D., Sader, J.E., Coleman, J.N. and Boland, J.J. Mechanical properties of individual electrospun polymer-nanotube composite nanofibers, *Carbon*, **47**(9) 2253-2258 (2009).
152. Manias, E., Touny, A., Wu, L., Strawhecker, K., Lu, B. and C.Chung, T. Polypropylene/montmorillonite nanocomposites. Re view of the synthetic routes and materials properties, *Chemistry of Materials*, **13**(10) 3516-3523 (2001).
153. Horrocks, A.R., Kandola, B.K., Smart, G., Zhang, S. and R.Hull, T. Polypropylene fibers containing dispersed clays having improved fire performance i. Effect of nanoclays on processing parameters and fiber properties., *Journal of Applied Polymer Science*, **106**(3) 1707-1717 (2007).
154. Uddin, F. Some aspects in textile nanofinishing,in proceedings the 86th textile institute world conference, the hong kong polytechnic university, november 2008.
155. Agic, A. and Mijovic, B. Mechanical properties of electrospun carbon nanotube composites, *Journal of the Textile Institute*, **97**(5) 419-427 (2006).
156. Horrocks, A.R., Kandola, B.K., Davies, P.J., Zhang, S. and Padbury, S.A. Developments in flame retardant textiles – a review, *Polymer Degradation and Stability*, **88**(1) 3-12 (2005).
157. Manias, E., Touny, A., Wu, L., Strawhecke, K., Lu, B. and Chung, T.C. Polypropylene/montmorillonite nanocomposites. Review of the synthetic routes and materials properties, *Chemistry of Materials*, **13**(10) 3516-3523 (2001).
158. Horrocks, Richard, A., Kandola, K., B., Smart, Gillian, Zhang, Sheng, Hull and Richard, T. Polypropylene fibers containing dispersed clays having improved fire performance. I. Effect of nanoclays on processing parameters and fiber properties, *Journal of Applied Polymer Science*, **106**(3) 1707-1717 (2007).
159. Joshi, M. and Viswanathan, V. High-performance filaments from compatibilized polypropylene/clay nanocomposites, *Journal of Applied Polymer Science*, **102**(3) 2164-2174 (2006).
160. Singh, K.V., Baton Rouge, L., Li, G. and Pang, S.-S. Applications and future of nanotechnology in textiles,applications and future of nanotechnology in textiles,” in proceedings of the 2006 beltwide cotton conferences, pp. 2498-2500, san arntonio,tex, USA.
161. Amir, M., Hasany, S.F. and Asghar, M.S.A. Modification of bentonite nanoclay for textile application, *Polimery*, **68**(2) 79-85 (2023).
162. najarzadeh, H. and montazer, m. Impact of nano-clay on improving the properties of cotton / nylon fabric, *Applied Nanomaterials and smart Polymers*, **1**(1) 29 - 37 (2023).
163. Jose, S., Shanmugam, N., Das, S., Kumar, A. and Pandit, P. Coating of lightweight wool fabric with nano clay for fire retardancy, *Journal of the Textile Institute*, **110**(5) 764-770 (2019).
164. Solariski, S., Mahjoubi, F., Ferreira, M., Devaux, E., Bachelet, P., Bourbigot, S., Delobel, R., Coszach, P., Murariu, M., Da silva Ferreira, A., Alexandre, M., Degee, P. and Dubois, P. (plasticized) polylactide/clay nanocomposite textile: Thermal, mechanical, shrinkage and fire properties, *Journal of Materials Science*, **42**(13) 5105-5117 (2007).
165. Asadi, M. and Montazer, M. Multi-functional polyester hollow fiber nonwoven fabric with using nano clay/nano TiO₂/polysiloxane composites, *Journal of Inorganic and Organometallic Polymers and Materials*, **23**(6) 1358-1367 (2013).
166. Maryan, A.S., Montazer, M. and Rashidi, A. Introducing old-look, soft handle, flame retardant, and anti-bacterial properties to denim garments using

- nano clay, *Journal of Engineered Fibers and Fabrics*, **8**(4) 68-77 (2013).
167. Abou El-Kheir, A., Abd El-Ghany, N., Fahmy, M., Aboras, S. and El-Gabry, L. Functional finishing of polyester fabric using bentonite nano-particles, *Egyptian Journal of Chemistry*, **63**(1) 85-99 (2020).
168. Bourbigot, S., Devaux, E. and Flambard, X. Flammability of polyamide-6/clay hybrid nanocomposite textiles, *Polymer Degradation and Stability*, **75** 397-402 (2002).
169. de Oliveira, C.R.S., Batistella, M.A., Lourenço, L.A., de Souza, S.M.d.A.G.U. and de Souza, A.A.U. Cotton fabric finishing based on phosphate/clay mineral by direct-coating technique and its influence on the thermal stability of the fibers, *Progress in Organic Coatings*, **150** (2021).
170. de Oliveira, C.R.S., Batistella, M.A., Guelli Ulson de Souza, S.M.A. and Ulson de Souza, A.A. Functionalization of cellulosic fibers with a kaolinite-tio(2) nano-hybrid composite via a solvothermal process for flame retardant applications, *Carbohydr Polym*, **266** 118108 (2021).
171. JOSHI, M., BHATTACHARYYA, A., AGARWAL, N. and PARMAR, S. Nanostructured coatings for super hydrophobic textiles, *Bulletin of Materials Science*, **35**(6) 933-938. (2012).
172. Farmahini-Farahani, M., Bedane, A.H., Pan, Y., Xiao, H., Eic, M. and Chibante, F. Cellulose/nanoclay composite films with high water vapor resistance and mechanical strength, *Cellulose*, **22**(6) 3941-3953 (2015).
173. Iman, M. and Maji, T.K. Effect of crosslinker and nanoclay on jute fabric reinforced soy flour green composite, *Journal of Applied Polymer Science*, **127**(5) 3987-3996 (2012).
174. Salih, W.K. Fire retardancy assessment of polypropylene composite filed with nano clay prepared from iraqi bentonite, *Journal of Physics: Conference Series*, **1003** (2018).
175. Mishra, K. and Vaidyanathan, R. The influence of nanoclay on the flame retardancy and mechanical performance of recycled carpet composites, *Recycling*, **4**(2) (2019).
176. Kertmen, N., Dalbaşı, E.S., KÖRİÜ, A., ÖZgÜNEY, A. and Yapar, S. A study on coating with nanoclay on the production of flame retardant cotton fabrics, *Tekstil ve Konfeksiyon*, **30**(4) 302-311 (2020).
177. Xue, J., Niu, Y., Gong, M., Shi, R., Chen, D., Zhang, L. and Lvov, Y. Electrospun microfiber membranes embedded with drug-loaded clay nanotubes for sustained antimicrobial protection, *ACS Nano*, **9** 1600-1612 (2015).
178. Qi, R., Guo, R., Zheng, F., Liu, H., Yu, J. and Shi, X. Controlled release and antibacterial activity of antibiotic-loaded electrospun halloysite/poly(lactico-glycolic acid) composite nanofibers, *Colloids Surf B Biointerfaces*, **110** 148-55 (2013).
179. Patel, S., Jammalamadaka, U., Sun, L., Tappa, K. and Mills, D.K. Sustained release of antibacterial agents from doped halloysite nanotubes, *Bioengineering (Basel)*, **3**(1) (2015).
180. Ghosh, A. Nano-clay particle as textile coating, *International Journal of Engineering & Technology IJET-IJENS*, **11**(5) 40-43 (2011).
181. Bouraada, M., Lafjah, M., Ouali, M.S. and de Menorval, L.C. Basic dye removal from aqueous solutions by dodecylsulfate- and dodecyl benzene sulfonate-intercalated hydrotalcite, *J Hazard Mater*, **153**(3) 911-8 (2008).
182. Cavani, F., Trifirò, F. and Vaccari, A. Hydrotalcite-type anionic clays: Preparation, properties and applications, *Catalysis Today*, **11** 173-301 (1991).
183. Gasser, M.S., Mekhamer, H.S. and Abdel Rahman, R.O. Optimization of the utilization of mg/fe hydrotalcite like compounds in the removal of sr(ii) from aqueous solution, *Journal of Environmental Chemical Engineering*, **4**(4) 4619-4630 (2016).
184. de Queiroga, L.N.F., França, D.B., Rodrigues, F., Santos, I.M.G., Fonseca, M.G. and Jaber, M. Functionalized bentonites for dye adsorption: Depollution and production of new pigments, *Journal of Environmental Chemical Engineering*, **7**(5) (2019).
185. Ogawa, M., Takee, R., Okabe, Y. and Seki, Y. Bio-geo hybrid pigment; clay-anthocyanin complex which changes color depending on the atmosphere, *Dyes and Pigments*, **139** 561-565 (2017).
186. Guillermin, D., Debroise, T., Trigueiro, P., de Viguierie, L., Rigaud, B., Morlet-Savary, F., Balme, S., Janot, J.-M., Tielens, F., Michot, L., Lalevee, J., Walter, P. and Jaber, M. New pigments based on carminic acid and smectites: A molecular investigation, *Dyes and Pigments*, **160** 971-982 (2019).
187. Yuan, J., Zhou, S., You, B. and Wu, L. Organic pigment particles coated with colloidal nano-silica particles via layer-by-layer assembly, *Chemistry of Materials*, **17** 3587-3594 (2005).
188. Dejoie, C., Martinetto, P., Dooryhée, E., Strobel, P., Blanc, S., Bordat, P., Brown, R., Porcher, F., Sanchez del Rio, M. and Anne, M. Indigo@silicalite: A new organic-inorganic hybrid pigment, *ACS Applied Materials & Interfaces*, **2**(8) 2308-2316 (2010).
189. Raha, S., Ivanov, I., Quazi, N. and Bhattacharya, S. Photo-stability of rhodamine-b/montmorillonite

- nanopigments in polypropylene matrix, *Applied Clay Science*, (2008).
190. Beltrán, M.I., Benavente, V., Marchante, V., Dema, H. and Marcilla, A. Characterisation of montmorillonites simultaneously modified with an organic dye and an ammonium salt at different dye/salt ratios. Properties of these modified montmorillonites and nanocomposites, *Applied Clay Science*, **97-98** 43-52 (2014).
 191. van der Linden, E.G., Malta, L.F.B. and Medeiros, M.E. Evaluation of synthetic routes to pigmentary grade bismuth vanadate, *Dyes and Pigments*, **90**(1) 36-40 (2011).
 192. Wang, X., Mu, B., Wang, W., Wang, Q. and Wang, A. A comparative study on color properties of different clay minerals/bio4 hybrid pigments with excellent thermal stability, *Applied Clay Science*, **181** (2019).
 193. Yi, J.Z. and Zhang, L.M. Removal of methylene blue dye from aqueous solution by adsorption onto sodium humate/polyacrylamide/clay hybrid hydrogels, *Bioresour Technol*, **99**(7) 2182-6 (2008).
 194. Momina, Mohammad, S. and Suzylawati, I. Study of the adsorption/desorption of mb dye solution using bentonite adsorbent coating, *Journal of Water Process Engineering*, **34** (2020).
 195. Hebeish, A.A., Shahin, A.A., Ragheb, A.A., Abd El-Thalouth, I., Allam, E.E. and Shaban, H.A. Innovation of radically new colorant hybrid nanocomposite for printing various textile fabrics, *Fibers and Polymers*, **20**(1) 69-79 (2019).
 196. Lertsutthiwong, P., Noomun, K., Khunthon, S. and Limpanart, S. Influence of chitosan characteristics on the properties of biopolymeric chitosan-montmorillonite, *Progress in Natural Science: Materials International*, **22**(5) 502-508 (2012).
 197. Umpuch, C. and Sakaew, S. Adsorption characteristics of reactive black 5 onto chitosan-intercalated montmorillonite, *Desalination and Water Treatment*, **53**(11) 2962-2969 (2013).
 198. Wang, W., Zhao, Y., Bai, H., Zhang, T., IbarraGalvan, V. and Song, S. Methylene blue removal from water using the hydrogel beads of poly(vinyl alcohol)-sodium alginate-chitosan-montmorillonite, *Carbohydrate Polymers*, **198** 518-528 (2018).
 199. Li, J., Cai, J., Zhong, L., Cheng, H., Wang, H. and Ma, Q. Adsorption of reactive red 136 onto chitosan/montmorillonite intercalated composite from aqueous solution, *Applied Clay Science*, **167** 9-22 (2019).
 200. Peng, Q., Liu, M., Zheng, J. and Zhou, C. Adsorption of dyes in aqueous solutions by chitosan-halloysite nanotubes composite hydrogel beads, *Microporous and Mesoporous Materials*, **201** 190-201 (2015).
 201. Vardikar, H.S., Bhanvase, B.A., Rathod, A.P. and Sonawane, S.H. Sonochemical synthesis, characterization and sorption study of kaolin-chitosan-TiO₂ ternary nanocomposite: Advantage over conventional method, *Materials Chemistry and Physics*, **217** 457-467 (2018).
 202. Dotto, G.L., Rodrigues, F.K., Tanabe, E.H., Fröhlich, R., Bertuol, D.A., Martins, T.R. and Foletto, E.L. Development of chitosan/bentonite hybrid composite to remove hazardous anionic and cationic dyes from colored effluents, *Journal of Environmental Chemical Engineering*, **4**(3) 3230-3239 (2016).
 203. Abukhadra, M.R., Adlii, A. and Bakry, B.M. Green fabrication of bentonite/chitosan@cobalt oxide composite (be/ch@co) of enhanced adsorption and advanced oxidation removal of congo red dye and Cr(VI) from water, *Int J Biol Macromol*, **126** 402-413 (2019).
 204. Wang, L. and Wang, A. Adsorption behaviors of congo red on the n,o-carboxymethyl-chitosan/montmorillonite nanocomposite, *Chemical Engineering Journal*, **143**(1-3) 43-50 (2008).
 205. Bée, A., Obeid, L., Mbolantenaina, R., Welschbillig, M. and Talbot, D. Magnetic chitosan/clay beads: A magnetic adsorbent for the removal of cationic dye from water, *Journal of Magnetism and Magnetic Materials*, **421** 59-64 (2017).
 206. Zhang, H., Ma, J., Wang, F., Chu, Y., Yang, L. and Xia, M. Mechanism of carboxymethyl chitosan hybrid montmorillonite and adsorption of Pb(II) and congo red by cmc-mmt organic-inorganic hybrid composite, *Int J Biol Macromol*, **149** 1161-1169 (2020).
 207. Yildirim, A. and Bulut, Y. Adsorption behaviors of malachite green by using crosslinked chitosan/polyacrylic acid/bentonite composites with different ratios, *Environmental Technology & Innovation*, **17** (2020).
 208. Zhao, Y., Kang, S., Qin, L., Wang, W., Zhang, T., Song, S. and Komarneni, S. Self-assembled gels of Fe-chitosan/montmorillonite nanosheets: Dye degradation by the synergistic effect of adsorption and photo-Fenton reaction, *Chemical Engineering Journal*, **379** (2020).
 209. Chang, M.Y. and Juang, R.S. Adsorption of tannic acid, humic acid, and dyes from water using the composite of chitosan and activated clay, *J Colloid Interface Sci*, **278**(1) 18-25 (2004).
 210. Pandey, S. and Mishra, S.B. Organic-inorganic hybrid of chitosan/organoclay bionanocomposites for hexavalent chromium uptake, *J Colloid Interface Sci*, **361**(2) 509-20 (2011).

-
211. Mokhtar, A., Abdelkrim, S., Djelad, A., Sardi, A., Boukoussa, B., Sassi, M. and Bengueddach, A. Adsorption behavior of cationic and anionic dyes on magadiite-chitosan composite beads, *Carbohydr Polym*, **229** 115399 (2020).